GENETICS

Supporting Information
http://www.genetics.org/lookup/suppl/doi:10.1534/genetics.114.162420/-/DC1

Modular Skeletal Evolution in Sticklebacks Is Controlled by Additive and Clustered Quantitative Trait Loci

Craig T. Miller, Andrew M. Glazer, Brian R. Summers, Benjamin K. Blackman, Andrew R. Norman, Michael D. Shapiro, Bonnie L. Cole, Catherine L. Peichel, Dolph Schluter, and David M. Kingsley

DOI: 10.1534/genetics.114.162420

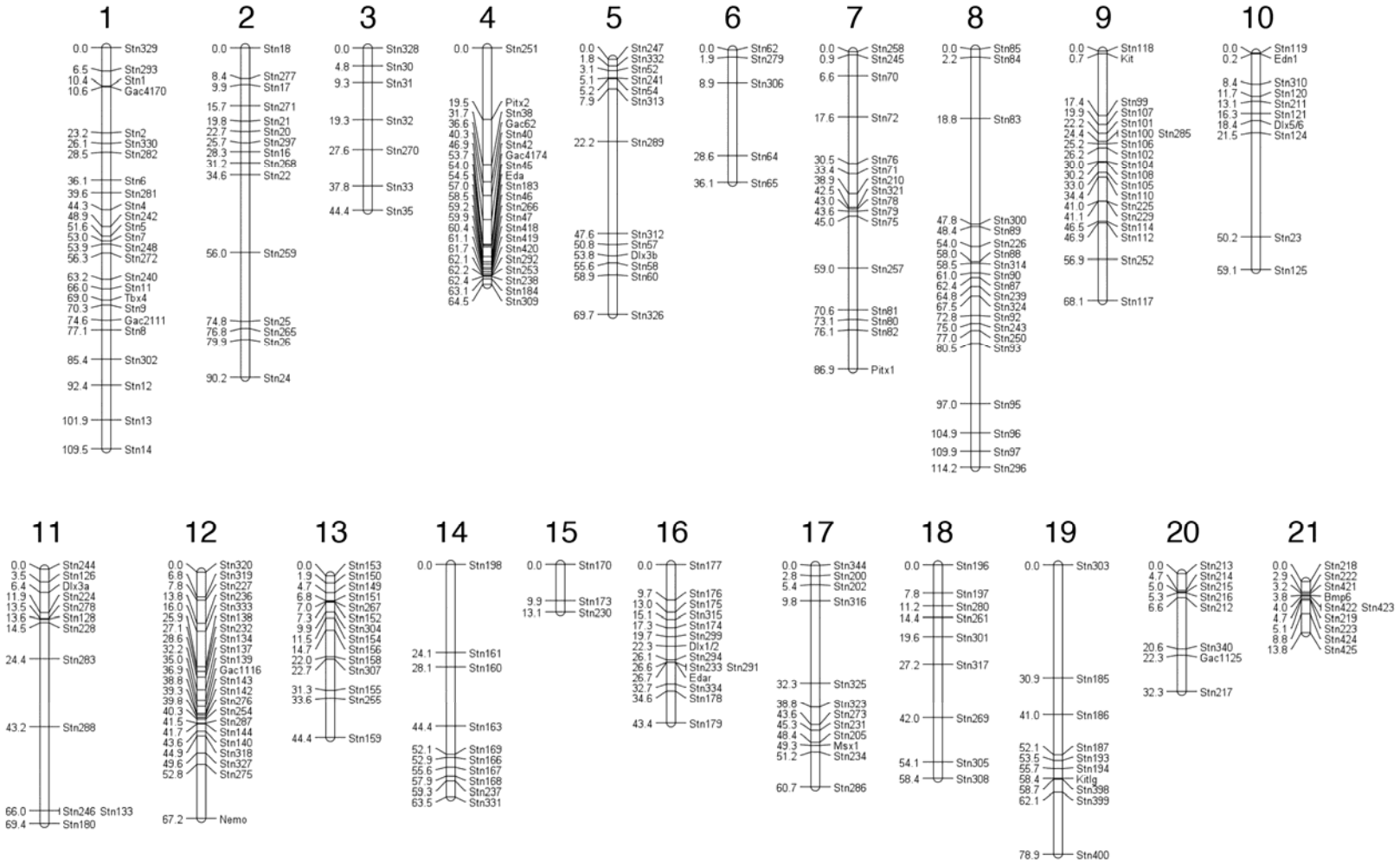

Figure S1 Genetic linkage map. The markers labeled on the map with gene names use the following nearby previously published (COLOSIMO *et al.* 2005; KNECHT *et al.* 2007a; MILLER *et al.* 2007; SHAPIRO *et al.* 2004) microsatellite markers: *Tbx4* = Stn221, *Pitx2*= Stn220, *Eda* = Stn365, *Pitx1*= Stn336, *Nemo* = Stn394, *Edar* = Stn337, *Kitlg* = Stn191 (since *Kitlg* does not recombine from Stn191 in this family). New markers labeled on the map with gene names use the following Stn markers and are described in Table S1 (*Bmp6* = Stn483, *Dlx1/2* = Stn339, *Dlx3a* = Stn430, *Dlx3b* = Stn427, *Dlx5/6* = Stn338, *Edn1* = Stn429, *Kit* = Stn428, *Msx1* = Stn343).

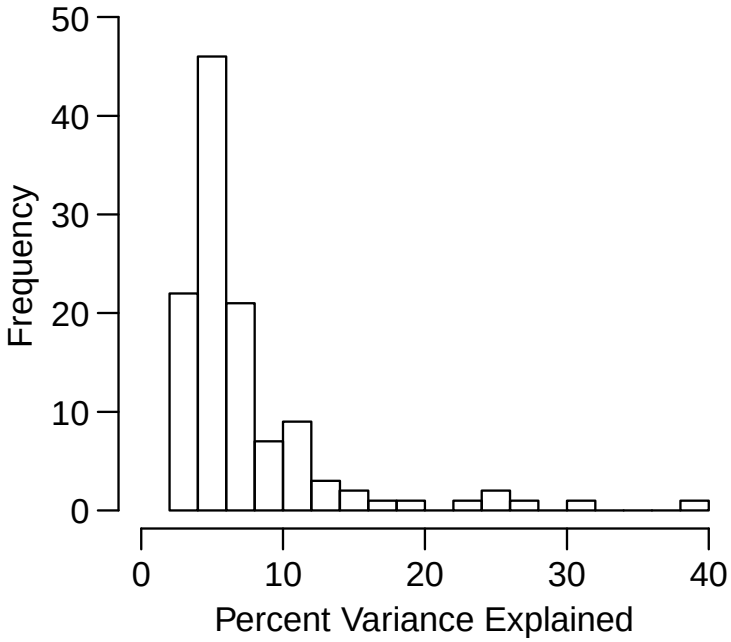

Figure S2 Distribution of percent variance explained (PVE). Histogram of PVE for the 118 filtered QTL. There are many QTL of small effect and few QTL of large effect.

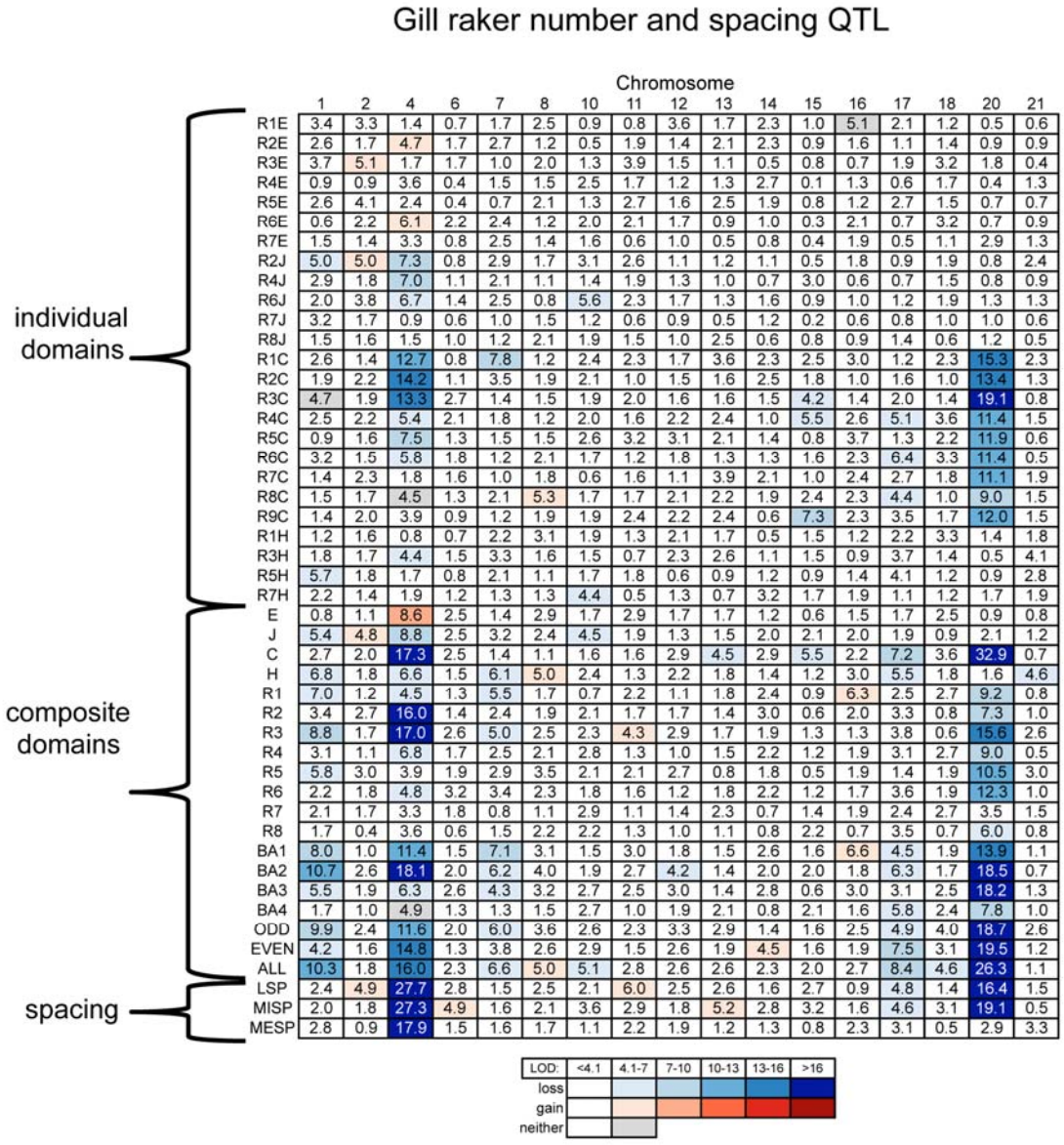

Figure S3 Heat map of gill raker QTL. Summary of LOD scores by phenotype for gill raker number and spacing QTL. Traits (abbreviations in Table S2) are listed to the left. Chromosomes with significant QTL detected are shown as columns. For each trait, the highest LOD score of any marker on each chromosome is shown, with LOD scores colored with the heat map shown at the bottom, with "gain" traits (where benthic allele confers more or bigger bones) colored red and "loss" traits (where benthic allele confers fewer or smaller bones) colored blue. Heterotic QTL (where homozygous marine and benthic F2 fish do not differ significantly in phenotype by two-tailed t-test) are shaded gray.

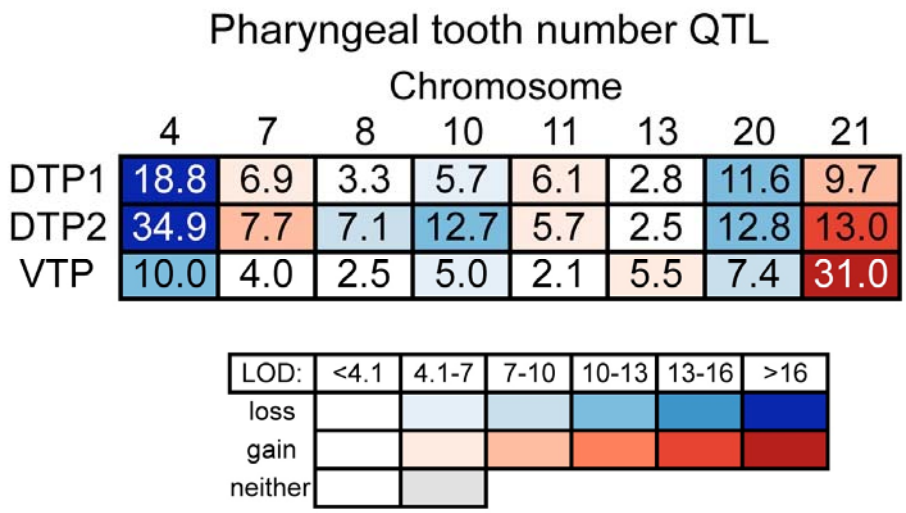

Figure S4 Heat map of pharyngeal tooth number QTL. Summary of LOD scores by phenotype for pharyngeal tooth number. Traits (abbreviations in Table S2) are listed to the left. Chromosomes with significant QTL detected are shown as columns. For each trait, the highest LOD score of any marker on each chromosome is shown, with LOD scores colored with the heat map shown at the bottom, with "gain" traits (where benthic allele confers more or bigger bones) colored red and "loss" traits (where benthic allele confers fewer or smaller bones) colored blue. Heterotic QTL (where homozygous marine and benthic F2 fish do not differ significantly in phenotype by two-tailed t-test) are shaded gray.

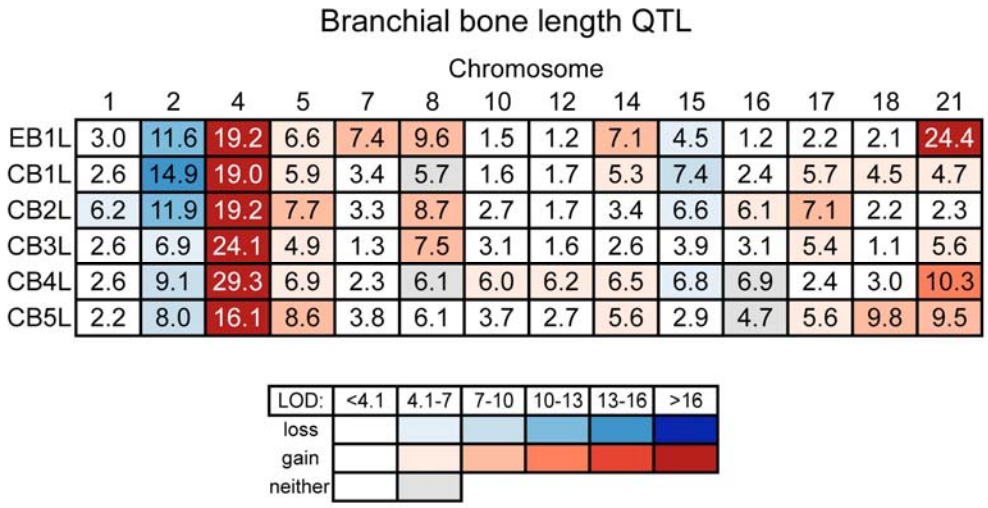

Figure S5 Heat map of branchial bone length QTL. Summary of LOD scores by phenotype for branchial bone length QTL. Traits (abbreviations in Table S2) are listed to the left. Chromosomes with significant QTL detected are shown as columns. For each trait, the highest LOD score of any marker on each chromosome is shown, with LOD scores colored with the heat map shown at the bottom, with "gain" traits (where benthic allele confers more or bigger bones) colored red and "loss" traits (where benthic allele confers fewer or smaller bones) colored blue. Heterotic QTL (where homozygous marine and benthic F2 fish do not differ significantly in phenotype by two-tailed t-test) are shaded gray.

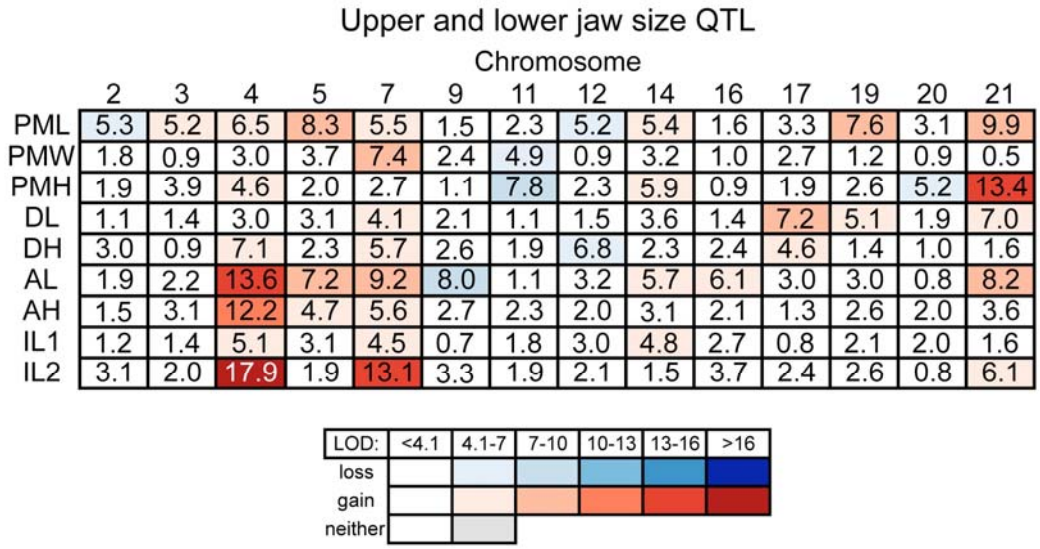

Figure S6 Heat map of jaw size QTL. Summary of LOD scores by phenotype for upper and lower jaw size QTL. Traits (abbreviations in Table S2) are listed to the left. Chromosomes with significant QTL detected are shown as columns. For each trait, the highest LOD score of any marker on each chromosome is shown, with LOD scores colored with the heat map shown at the bottom, with "gain" traits (where benthic allele confers more or bigger bones) colored red and "loss" traits (where benthic allele confers fewer or smaller bones) colored blue. Heterotic QTL (where homozygous marine and benthic F2 fish do not differ significantly in phenotype by two-tailed t-test) are shaded gray.

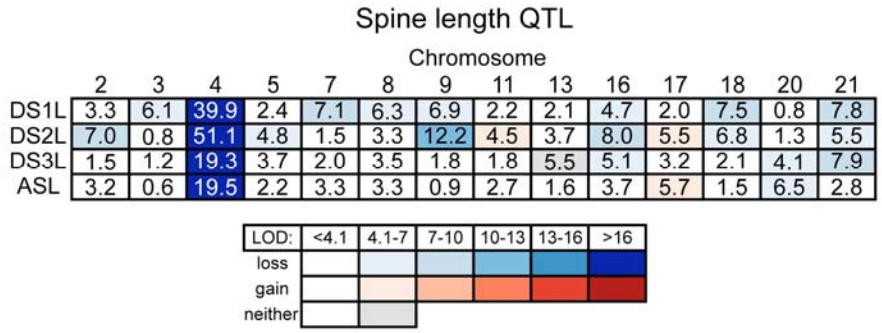

Figure S7 Heat map of spine length QTL. Summary of LOD scores by phenotype for spine length QTL. Traits (abbreviations in Table S2) are listed to the left. Chromosomes with significant QTL detected are shown as columns. For each trait, the highest LOD score of any marker on each chromosome is shown, with LOD scores colored with the heat map shown at the bottom, with "gain" traits (where benthic allele confers more or bigger bones) colored red and "loss" traits (where benthic allele confers fewer or smaller bones) colored blue. Heterotic QTL (where homozygous marine and benthic F2 fish do not differ significantly in phenotype by two-tailed t-test) are shaded gray.

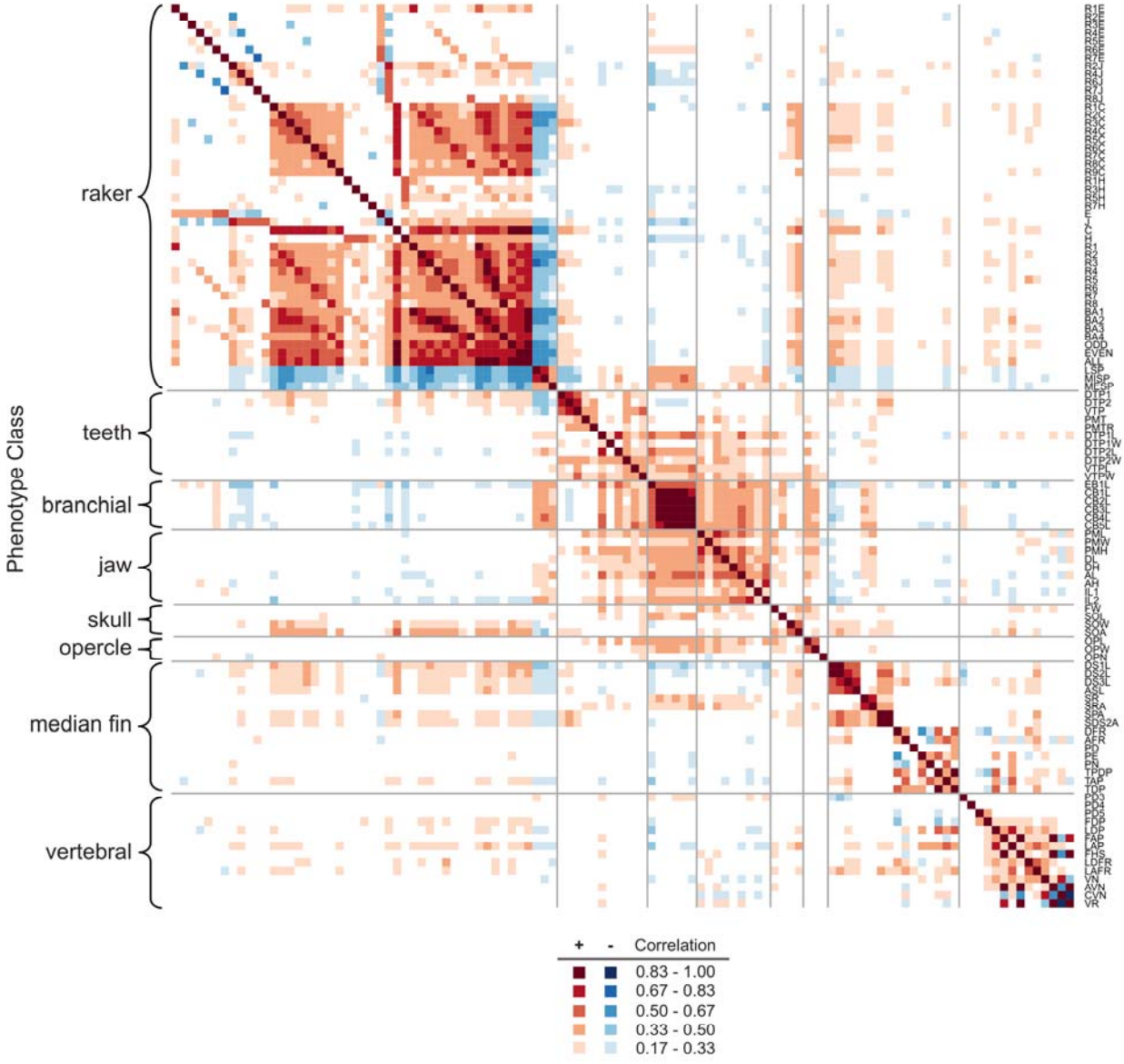

Figure S8 Trait covariance heat map. Classes of traits are grouped on the left, and abbreviations (defined in Table S2) of individual traits are listed on the right. For each pair of traits, the covariance of Z-scored phenotypes (correlation) is indicated by the heat map shown at bottom, with positive covariances colored red and negative covariances colored blue.

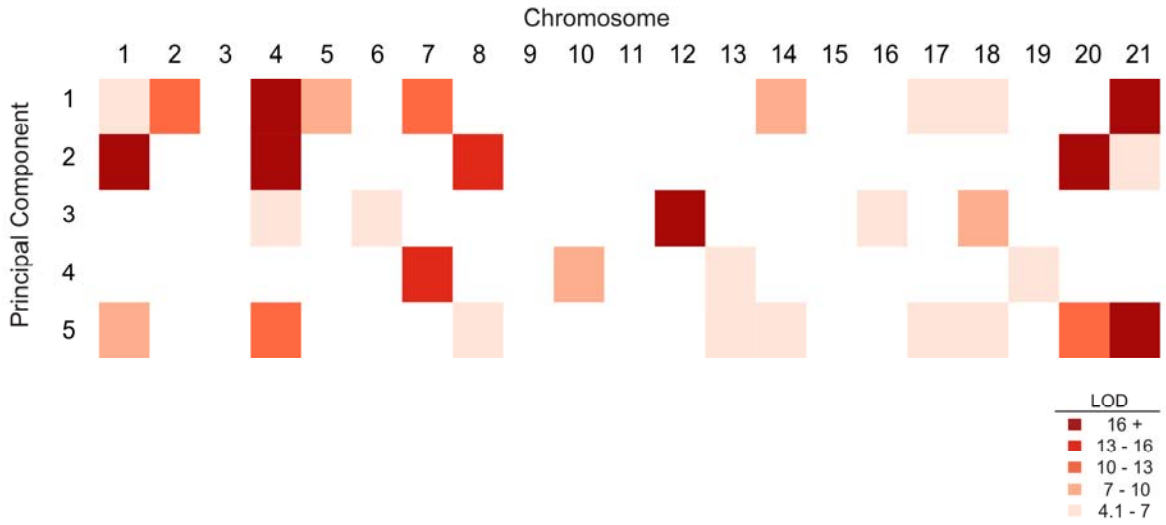

Figure S9 Genome-wide overview of principal component QTL. For each of the top five principal components, the LOD score for each significant QTL is indicated by the heat map shown in the bottom right. Further details of the QTL are presented in File S4.

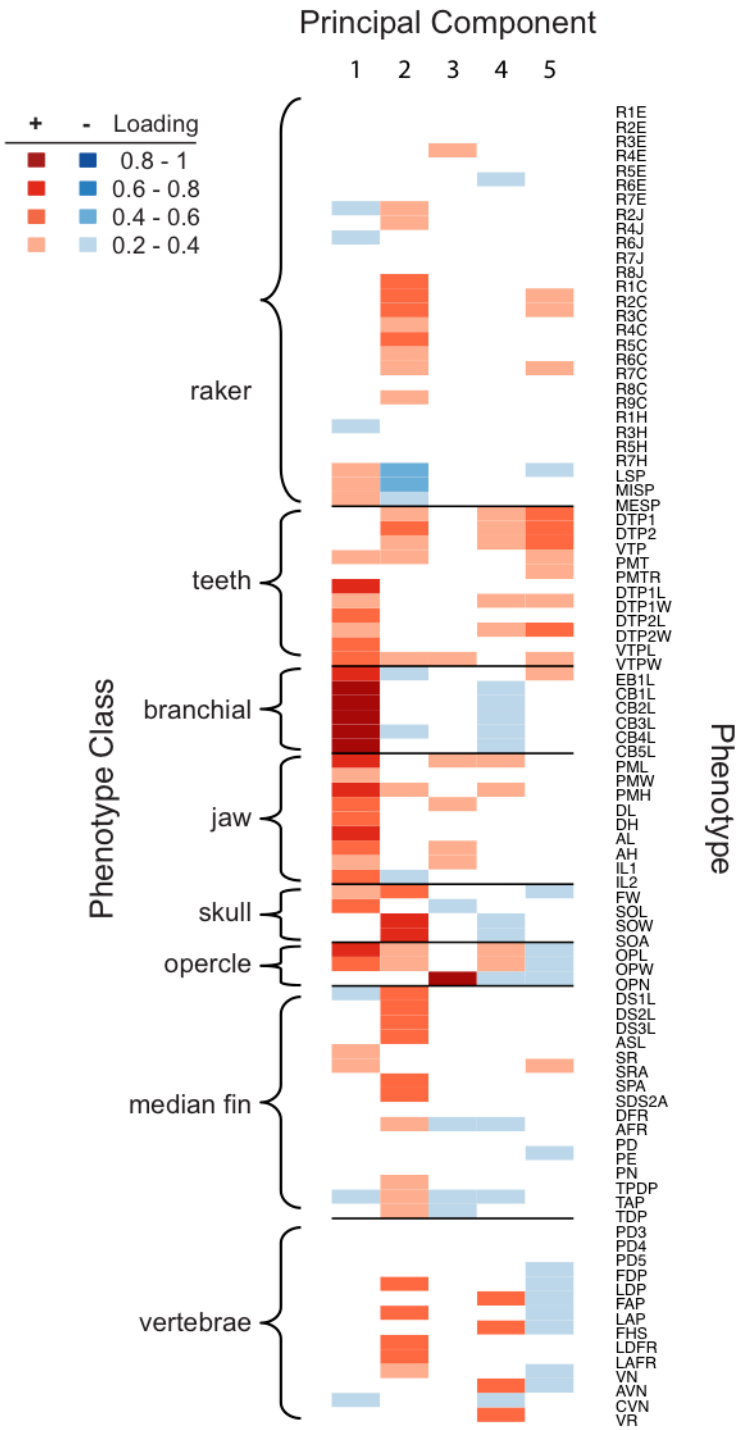

Figure S10 Trait loadings for top five principal components. Classes of traits are grouped on the left, and abbreviations (defined in Table S2) of individual traits are listed on the right. For each principal component, the loading for each trait is indicated by the heat map shown in the upper left, with positive loadings colored red and negative loadings colored blue.

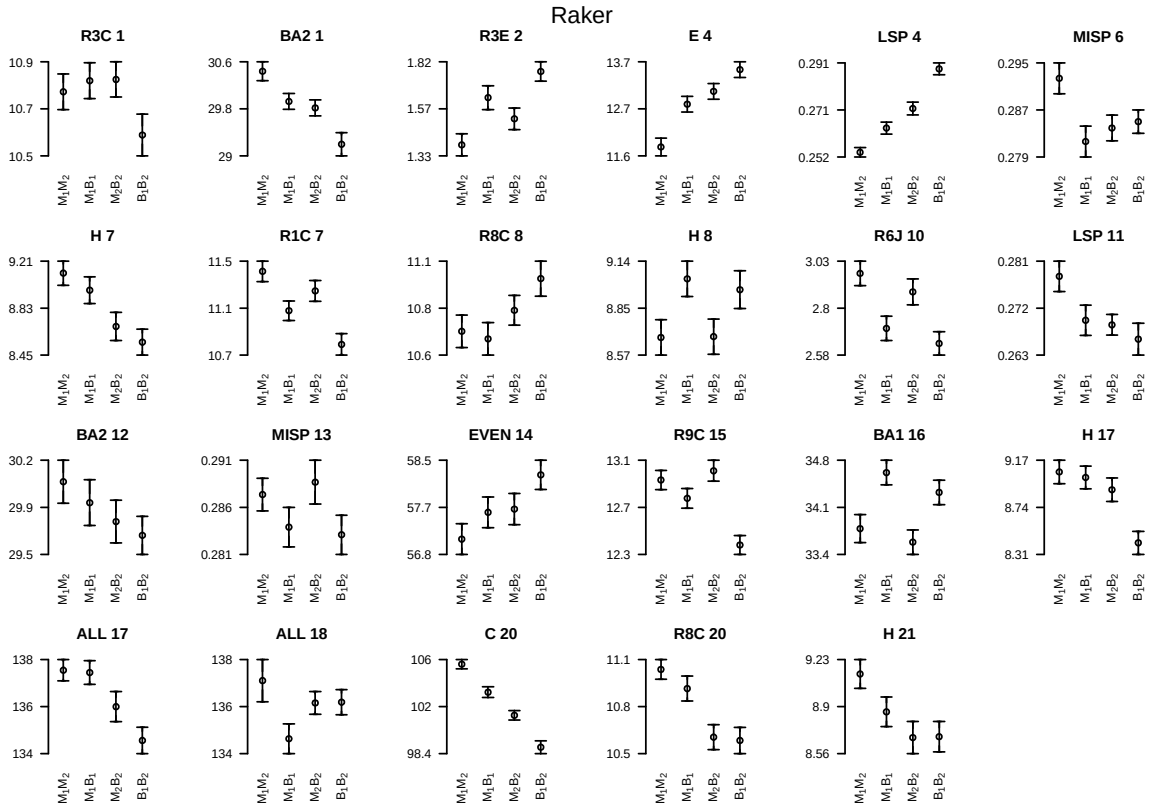

Figure S11 Mean trait phenotypes for different genotypes at peak marker for individual gill raker QTL. Each plot shows the mean size and sex corrected phenotype, if appropriate (back-transformed to a fish of 40 mm), and standard error of the mean for each genotypic class of F2 fish. See Table S2 for list of trait abbreviations, and Table S4 for peak markers used to define genotypic classes at corresponding QTL. Genotype abbreviations: M_1M_2 = homozygous marine, M_1B_1 and M_2B_2 = heterozygous marine/benthic, B_1B_2 = homozygous benthic.

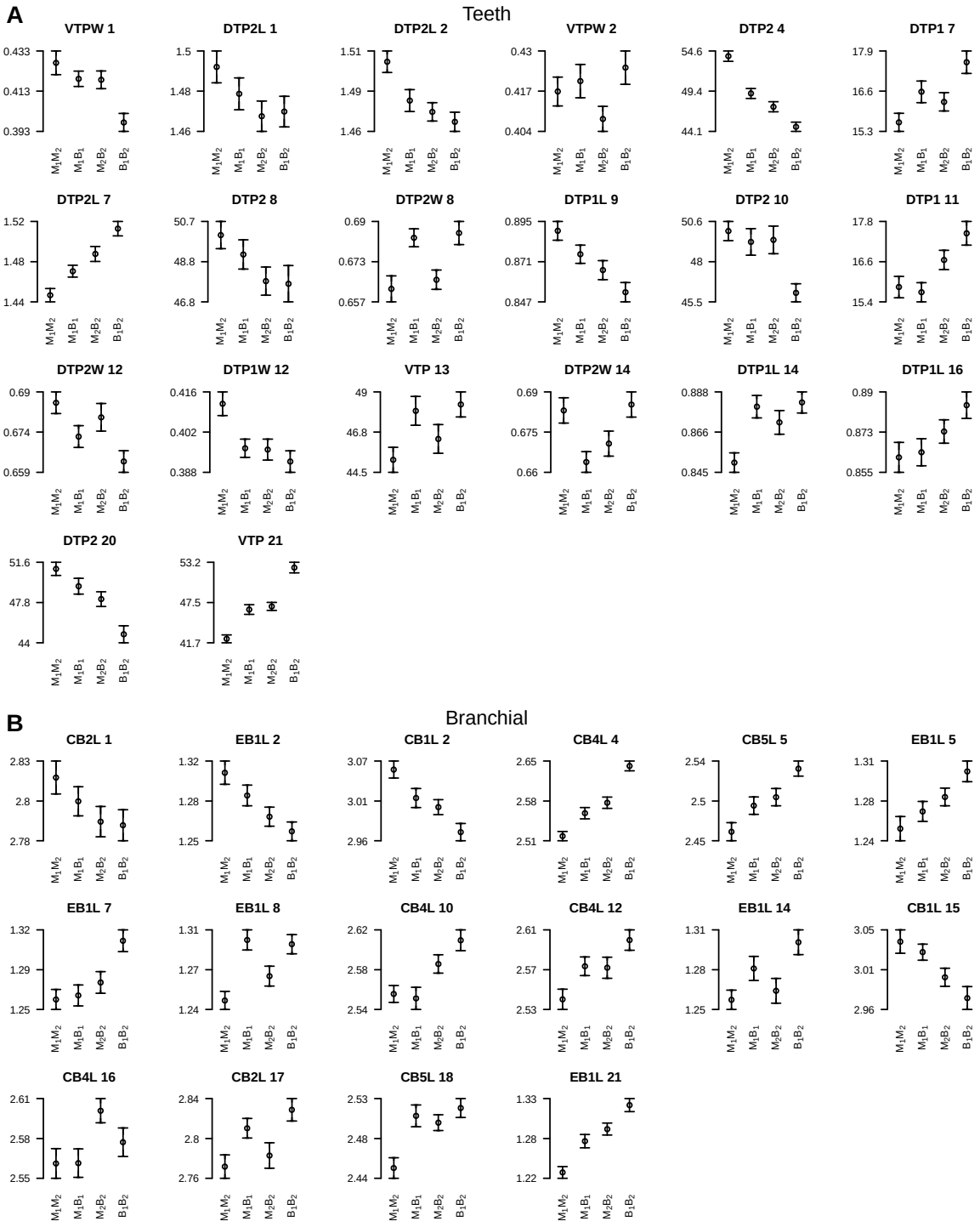

Figure S12 Mean trait phenotypes for different genotypes at peak marker for individual teeth (A) and branchial bone (B) QTL. Each plot shows the mean size and sex corrected phenotype, if appropriate (back-transformed to a fish of 40 mm), and standard error of the mean for each genotypic class of F2 fish. See Table S2 for list of trait abbreviations, and Table S4 for peak markers used to define genotypic classes at corresponding QTL. Genotype abbreviations: M_1M_2 = homozygous marine, M_1B_1 and M_2B_2 = heterozygous marine/benthic, B_1B_2 = homozygous benthic.

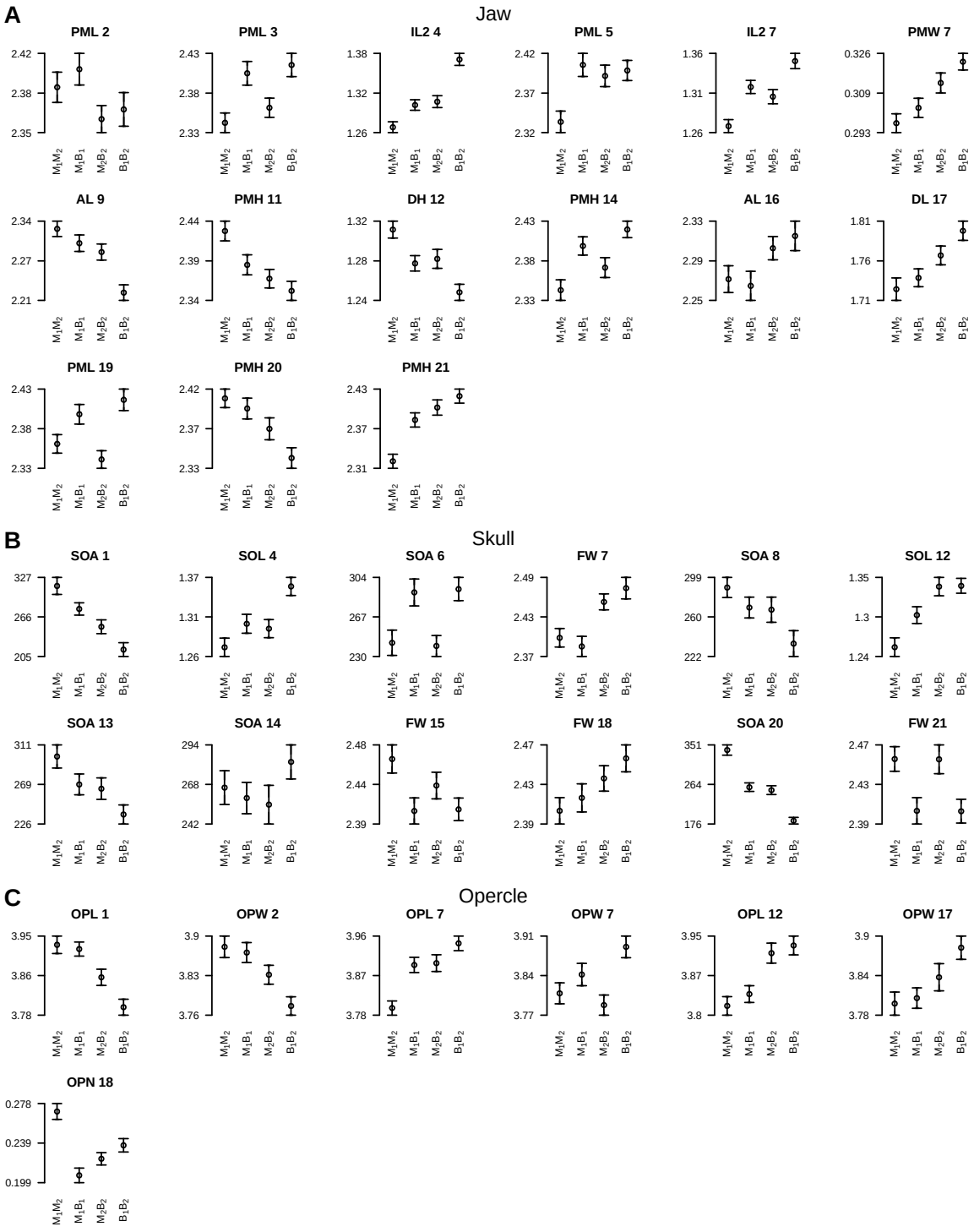

Figure S13 Mean trait phenotypes for different genotypes at peak marker for individual jaw (A), skull (B), and opercle (C) QTL. Each plot shows the mean size and sex corrected phenotype, if appropriate (back-transformed to a fish of 40 mm), and standard error of the mean for each genotypic class of F2 fish. See Table S2 for list of trait abbreviations, and Table S4 for peak markers used to define genotypic classes at corresponding QTL. Genotype abbreviations: M_1M_2 = homozygous marine, M_1B_1 and M_2B_2 = heterozygous marine/benthic, B_1B_2 = homozygous benthic.

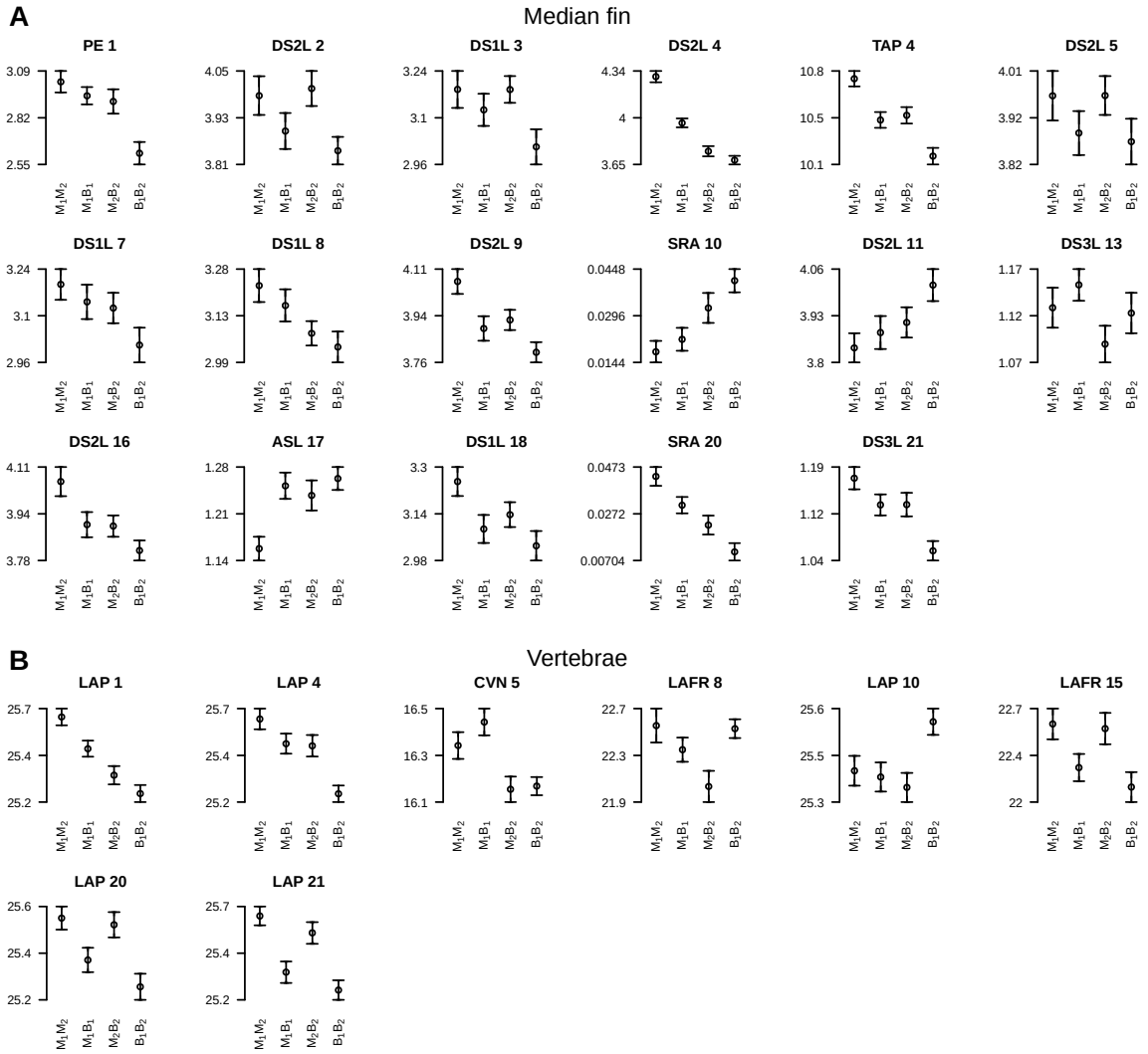

Figure S14 Mean trait phenotypes for different genotypes at peak marker for individual median fin (A) and vertebrae (B) QTL. Each plot shows the mean size and sex corrected phenotype, if appropriate (back-transformed to a fish of 40 mm), and standard error of the mean for each genotypic class of F2 fish. See Table S2 for list of trait abbreviations, and Table S4 for peak markers used to define genotypic classes at corresponding QTL. Genotype abbreviations: M_1M_2 = homozygous marine, M_1B_1 and M_2B_2 = heterozygous marine/benthic, B_1B_2 = homozygous benthic.

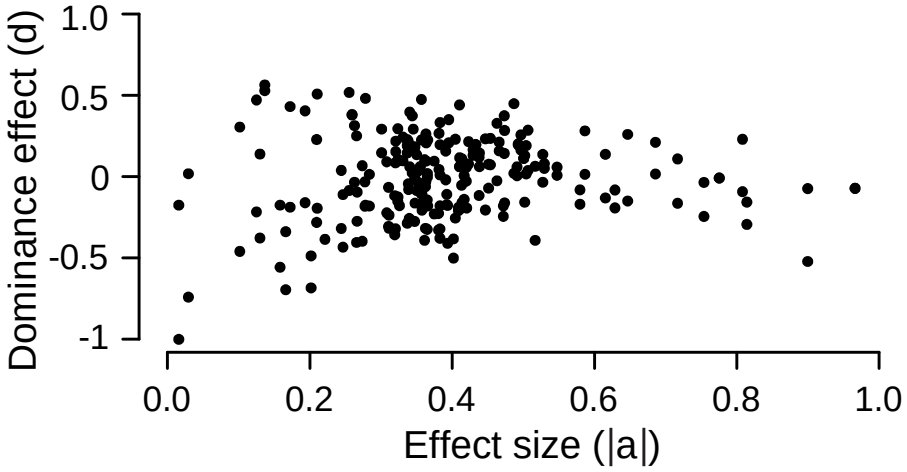

Figure S15 Relation between dominance (*d*, y-axis) and absolute value of *a,* the additive coefficient (x-axis). The range of observed *d* values appears greater with smaller effect sizes.

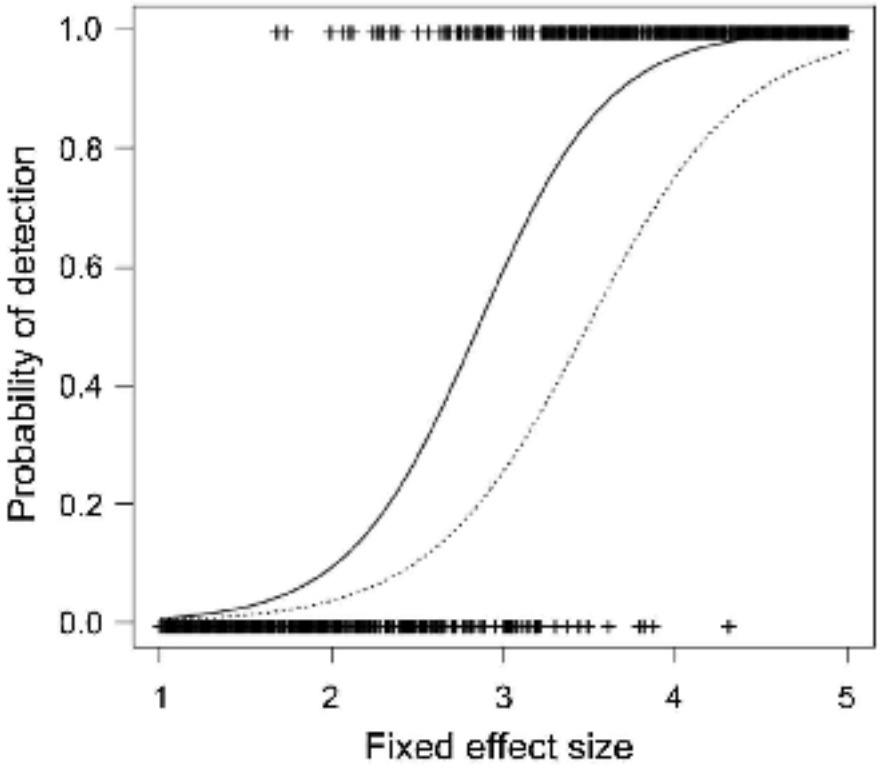

Figure S16 Probability of detection of QTL for simulated varying effect sizes. Logistic regressions fitted to the 400 data points on detection (0 = no, 1 = yes), showing probability of detection for QTL with dominance (*d/a*) of 1 (dominant, solid curve) or 0 (additive; dashed curve). Additive QTL are less likely to be detected.

File S1

Supplemental Materials and Methods

Grandparental population phenotyping

Skeletal morphologies of Japanese marine and Paxton benthic adult wild fish were compared by micro-computerized tomography using a Scanco uCT 40 scanned at 55kvp, 145 uA, at high resolution averaging four frames.

Phenotyping skeletal traits in F2 fish

We phenotyped 110 skeletal traits using a variety of methods described below. All traits were quantified on the left side, except for (1) premaxilla height and length which were quantified on the right side, and (2) premaxilla width, frontal width, supraoccipital traits, median fin and vertebral position traits, which are bilateral or midline measurements (see Figure 2). All linear measurements were quantified using an eye reticule on a Nikon SMZ1500 dissecting microscope unless noted otherwise.

Dissection method for branchial trait phenotyping

We developed a method to dissect out the entire branchial skeleton and mount it flat on a coverslip (Figure 2A). Briefly, under a Zeiss STEMI 2000 dissecting microscope with watchmaker's forceps, eyes were removed, and four cuts were made with iris or vannas scissors: two bilateral cuts dorsal to the opercle and hyomandibula through to the eye sockets, a cut across the frontal bone through the eye sockets, and a cut through the midline parasphenoid bone. Ventrally, the ceratohyals were disarticulated from the basihyal, and the urohyal removed. Next, the entire facial skeleton was removed, exposing the branchial skeleton. The epibranchials were detached from the neurocranium and the branchial skeleton removed by pulling the gut tube away from the rest of the fish. Soft tissue including the gut was removed and a single midline incision was made between the dorsal tooth plates to allow mounting the branchial skeletons flat on bridged coverslips as in Figure 2A. This method enables visualization of the entire branchial skeletal pattern from a dorsal view, as well as previously described variation in the pigmentation of the gill filaments from a ventral view (MILLER *et al.* 2007).

Gill raker traits

Along the anterior/posterior axis, gill rakers are distributed across nine rows projecting from both the anterior and posterior faces of all five branchial segments, except for the fifth branchial segment, which has only an anterior row (Figure 2A). Using the edge of Alizarin-positive branchial bone staining, we defined four dorsal-ventral raker domains as follows: (1) hypo (all rakers medial to the ceratobranchial), (2) cerato (bounded by the edges of the ceratobranchial bones), (3) joint (between

epibranchial and ceratobranchial), and (4) epi (dorsal to the epibranchial) (Figure 2B-E). If a raker spanned these bone landmarks, the center of the raker base was used to assign each raker to a domain. We recorded raker number in each of these 25 anterior-posterior and dorsal-ventral domains using a Zeiss STEMI 2000 dissecting microscope. We also combined the individual domain phenotypes into 19 composite phenotypes in the following possible developmental modules: rows, segments (branchial arches), odd rows, even rows, all, and dorsal/ventral domains (hypo, cerato, joint, and epi).

In addition to gill raker number, we directly measured the inter-raker spacing distance at three positions (lateral, middle, and medial, Figure 2F) along row 2 rakers. Lateral spacing was measured between the second and third raker from the ceratobranchial-epibranchial joint, middle spacing was measured between two rakers in the middle of the ceratobranchial, and medial spacing was measured between the second and third raker from the hypobranchial-ceratobranchial joint. All three spacing measurements were made between the center of the base of the two rakers being measured. For all three spacing measurements, if an atypical raker spacing was present following the above landmarks, an adjacent raker space was recorded if it appeared more typical of the spacing within the row.

We phenotyped gill raker length (from raker tip to ceratobranchial bone of the third raker from the ceratobranchial/epibranchial joint in rows 1 and 2), but after no significant genetic effect was detected after scoring 92 F2 males, we did not pursue this trait further.

Pharyngeal dentition

We quantified pharyngeal tooth number on all three pharyngeal toothplates: the two dorsal toothplates (DTP1 and DTP2) attached to the pharyngobranchials (ANKER 1974), and the one ventral pharyngeal toothplate (VTP) attached to the fifth ceratobranchial (Figure 2G). Teeth were counted using a Zeiss Axiophot compound microscope with DIC optics. Baby teeth that were visible under DIC but did not stain with Alizarin red were not counted. In addition, we measured the lengths and widths of all three toothplates (Figure 2H) by recording the longest and widest point-to-point measurements between Alizarin-positive toothplate bone.

Branchial bones

Along the dorsal-ventral axis, the branchial skeleton consists of: four epibranchials (EBs, dorsal bones in the roof of the buccal cavity); five ceratobranchials (CBs, long ventral bones in the floor of the buccal cavity), and three hypobranchials (HBs, short ventral bones in between the ceratobranchials and the midline). We measured the lengths of all five ceratobranchials and the first epibranchial using the two anterior corners of Alizarin-positive bone as landmarks (see Figure 2I). The lengths of the highly

three-dimensional epibranchials 2-4 and the widths of all ceratobranchials and epibranchials were not measured due to marked variation in mounting angles.

Jaw traits

Premaxillas were manually removed then soaked for several minutes in a dilute 2.5% bleach solution to remove soft tissue before measuring height, width, and length as in Figure 2J. Lower jaw measurements were quantified by dissecting out and separating the left dentary and articular as in Figure 2K, acquiring digitized images with an Evolution MP camera using ImageProPlus on a Leica MZFLIII microscope, then using ImageProPlus software to make linear measurements as in Figure 2K,L.

Skull and opercle traits

We quantified four skull traits: the linear measurement of frontal width or interorbital distance (Figure 2M), and three measurements of the supraoccipital crest (Figure 2N). Supraoccipital traits were quantified from digital images of the dorsal view of the skull taken with an Evolution MP camera on a Leica MZFLIII microscope and analyzed with ImageProPlus software. Three measurements of opercle size and shape were made: the length and width of the opercle, and a measurement of the width of the neck of the opercle (Figure 2O).

Median fin and vertebral traits

Spine serrations were scored from digital images of the second dorsal spine acquired with a Nikon D1X camera fixed to a Nikon SMZ-U microscope. Area of the anterior surface of the spine was calculated by counting the number of pixels in Photoshop (Adobe) and converting to square millimeters. The serration area (SRA) was calculated by subtracting a digitally smoothened dorsal spine area (i.e., a spine without serrations, SDSA) from the total spine area (SPA, Figure 2P). Pterygiophore and fin ray number, and anal spine lengths were quantified under a Leica S8APO microscope with an eye reticule. For all vertebral traits, animals were first X-rayed (Figure 2Q) at 5x magnification for 15-20 seconds at 20 kV in a Micro–50 cabinet specimen radiography machine (Faxitron). Positions of bones in the median skeleton were assigned a numerical value corresponding to the closest vertebra as described (Ahn and Gibson 1999). The position of the last dorsal and anal fin ray was determined based on the position of the pterygiophore that supported the fin ray. On occasion, the element was judged to be equidistant from two vertebrae and was assigned a value that was an average of the two vertebrae.

Genome-wide linkage map

Linkage map construction

A set of 275 microsatellites was genotyped in a single full-sibling family ("Family 4") of 370 fish from a Japanese marine (JAMA) by Paxton benthic (PAXB) freshwater F2 cross (COLOSIMO *et al.* 2004). These markers consisted of previously described sets of genome-wide microsatellites (ALBERT *et al.* 2008; COLOSIMO *et al.* 2004; PEICHEL *et al.* 2001) and markers near previously mapped genes (COLOSIMO *et al.* 2005; KNECHT *et al.* 2007b; MILLER *et al.* 2007; SHAPIRO *et al.* 2004). In addition, we added 16 new markers to the genetic map by genotyping new microsatellites near candidate genes with important roles in pharyngeal arch patterning in other vertebrates (*Dlx1/2*, *Dlx5/6*, *Dlx3*, *Msx1*, *Edn1*) as well as new positional markers. New markers were identified using a variety of methods including degenerate PCR, bacterial artificial chromosome (BAC) screening by radioactively labeled overgo hybridization, BAC end sequencing, physical map information, and publicly available previously sequenced BAC ends, as described in Supplemental Tables S1 and below. A linkage map (Figure S1) was constructed with JoinMap 3.0 (Kyazma), using previously described settings (PEICHEL *et al.* 2001) but by accepting more conservative LOD 6 groupings. The total map length is 1287.8 cM over 21 linkage groups, resulting in an average marker spacing of 5.1 cM. For each linkage group, proper phase was determined from the grandparental genotypes.

Cloning Dlx and Msx genes

Intergenic (*Dlx5/*6) or genic (*Msx1*, *Dlx3a*, and *Dlx3b*) regions of new genes added to map were amplified by PCR using the following primers (all sequences 5' to 3'). For *Dlx5/6,* PCR primers GGTGGGAAAGTGTTTGCACACC and CTGAGACAATCCGCATTCCTGTGG were designed to conserved intergenic sequences (ZERUCHA *et al.* 2000) which were found to flank Stn339 in intervening genomic sequence. For *Dlx3a* and *Dlx3b*, portions of two stickleback *Dlx3* genes were amplified and sequenced using a common forward degenerate primer (GGGTGAAGATHTGGTTYCARAA) and a reverse degenerate primer for either *Dlx3a* (CGGGCTGRTACCARTTYTGRTG) or *Dlx3b* (CGCCCTGYTGRTACCARTGRTT). The resulting *Dlx3* sequences were used to design two gene specific overgoes (see below) for BAC screening. Both *Dlx5/6* and *Dlx3* PCRs used Little Campbell marine genomic DNA as a template. For *Msx1,* degenerate RT-PCR primers CCGTTCAGCGTCGARGCNCTNATGGC and GGGGTGRTACATRCTRTANCC were used with oligo-dT reverse primed cDNA harvested from a 1 cM long Little Campbell marine fry. The resulting RT-PCR amplicon sequence was used to design overgoes (see below) for BAC screening.

Overgo screening, BAC end sequencing, and genotyping

Overgo screening was performed as described at www.chori.org/bacpac/overgohyb.htm. *Dlx1/2* overgoes were directly designed to conserved intergenic sequence (GHANEM *et al.* 2003). Forward and reverse overgo sequences (5' to 3') for each marker or gene were: *Msx1*:
CGGTAGTCTGGATACTTCAGTTCC and GCCCATCGATAAAGCAGGAACTGA; Stn207: TTTCAGCAGGTGCAACGTTTCCAC and AACTAAGAAGGCGAGCGTGGAAAC; *Dlx1/2:* ACCAAGATCTCGAGTGCACAATGT and CCTCATTACGCTGATGACATTGTG; *Dlx3a*: GGCGGCAGTATTAAGAGTAATGCG and CGGTGGGATCCACAAGCGCATTAC; *Dlx3b*: CCGACGCACAGCTCGTCGCCGCCA and TATAATCCTCCAGGTATGGCGGCG; Stn48: GTGCCAGAAAACTTGCATTCCAGG and ATCCCCTCACGTCACACCTGGAAT; EaccMgtg: GCAGGGTGATTGAATGTCTTCACT and GTCCTTAGGAAGATGCAGTGAAGA; 48B15.t7: AACAGTGTTGAGCGCTGAAATGCC and ACCTGTATGCACACACGGCATTTC; Stn292:
AAGATACGGGCTGATGAGCAGTGA and TTCTTACTACGCCTCCTCACTGCT; Stn222: TCGCACTTCAGACACTAAGCCTTG and TGAAGGGTGTCCAAACCAAGGCTT; Bmp6: TGTGACGTTGACCTCAGCTAGACT and GAGGATTTAAACCGGGAGTCTAGC.
For overgo screening, three pairs of labeled overgoes were combined in one hybridization bottle containing four filters, and positive BACs subsequently identified using a combination of the physical map (KINGSLEY *et al.* 2004) and PCR screening. BAC ends were sequenced using ABI3730xl manufacturer's suggestions, using 8 uL of ABI BigDye per 20uL sequencing reaction. Genotypes were generated essentially as previously described (MILLER *et al.* 2007; PEICHEL *et al.* 2001).

QTL mapping and analyses

Trait transformations

Trait processing and analysis was performed in R (http://www.R-project.org/). A custom pipeline was made to correct each trait for sex and/or size-dependence, log-transform if appropriate, and to remove phenotypic outliers as follows. First each trait was tested for size dependence by linear regression vs. standard length (SL), for sex dependence by a one-way ANOVA using sex as a factor, and for sex and size dependence using SL as a covariate and sex as a main effect in a General Linear Model (GLM) ANOVA. If the trait was neither sex nor size dependent, raw trait values were used for QTL mapping. If there was SL-dependence but no sex-dependence, traits were regressed against SL to obtain residuals. If there was sex-dependence but not size dependence, sex was corrected for using the residuals of a one-way ANOVA with sex as a factor. If traits were significantly dependent upon both sex and size, the residuals of the GLM ANOVA were used for QTL mapping. Outliers (defined as fish that had trait values greater than four standard deviations from the mean trait value) were removed and ANOVAs, regressions, and GLM ANOVAs were redone without outliers. Outliers were rare and consisted of only 35 values for 17 total traits (AH, DH, DL, DS1L, DS2L, FDP, IL1, IL2, OPL, OPN, PD4, PML, PMW, SDS2A, SOL, SPA, and SRA). Traits were log-transformed when the

transformation equalized variances (in sextiles ranked by standard length) by Levene's test for equality of variances, and/or normalized the residuals by an Anderson-Darling test of normality.

QTL mapping

QTL mapping was performed in R/qtl (BROMAN and SEN 2009). Initial QTL mapping was performed with *scanone* with Haley-Knott regressions (hk). For each phenotype, ten thousand permutations were performed to determine a LOD threshold at which alpha equals 0.05. The average of these trait-specific thresholds was 4.1; thus this value was used as the QTL significance threshold for all traits. All significant QTL by *scanone* were also identified by *stepwise* mapping, so the larger *stepwise* set of QTL are presented here. The *stepwise* algorithm was performed by an automated forward-backward stepwise search for QTL using *stepwiseqtl* with a main penalty of 4.1, which was the average penalty from 100 *scantwo* permutations for each trait. QTL peak markers and LOD scores were calculated using *refineqtl* and percent variances explained were calculated with *fitqtl*. For a small number of traits (n=11), the *stepwiseqtl* output included markers with a LOD less than 4.1. These markers were conservatively removed. In 10 cases, the *stepwiseqtl* output included two markers on the same chromosome. Only cases where both peak markers had LODs greater than 4.1 and also had non-overlapping 1.5 LOD intervals were considered as two QTL. In cases where the two linked markers had overlapping 1.5 LOD intervals, only the peak marker with the highest LOD was considered a QTL. LOD scores for QTL on chromosomes that did not have significant effects were determined with *addqtl*, adjusting for QTL that were identified from the stepwise search. Additional QTL were included from *addqtl* if they surpassed a 4.1 LOD score threshold and LODs were recalculated as above. This *addqtl/refineqtl/fitqtl* process was iteratively repeated for three rounds and all QTL that had a LOD score above 4.1 in the final *fitqtl* model were included in the final QTL set. LOD scores for phenotypes with no significant QTL were determined by *scanone* with Haley-Knott regressions. Heat maps in Figures 3 and S2-S6 use color schemes from http://colorbrewer2.org/.

Anatomical specificity of QTL

For investigating the anatomical specificity of QTL (Figure 4), the subset of QTL with clearly or likely serially homologous domains (QTL in the raker, teeth, branchial, jaw, and spine classes) were considered. QTL controlling raker spacing were excluded because this phenotype was only quantified on one segment, and QTL controlling toothplate size and tooth number were analyzed separately.

Principal Components Analysis

To determine the major axes of skeletal variation in the dataset, we performed Principal Components Analysis (PCA) using the *FactoMineR* package in R. Phenotypes were size/sex/log-adjusted as necessary (see Table S2) and Z-scored. Missing data were imputed using the *imputePCA* command, then weighted PCA was performed using phenotype weights such that the total weight for each phenotype class was equal. We performed PCA on all phenotypes, excluding composite phenotypes where the non-composite phenotypes comprising the composite phenotype were also present. The first five principal components explained 18.4, 9.4, 4.9, 4.6, and 4.4 percent of the phenotypic variance, respectively. The coordinates for each fish for the five largest principal components were extracted and QTL were mapped as described above.

Investigating biases in dominance

For simulations investigating QTL detection biases for dominance, two cases of QTL were compared: dominant QTL (d/a=1; heterozygotes have the same mean phenotype as the benthic B_1B_2 genotype) and additive QTL (d/a=0; heterozygous mean phenotype equals the mean of the M_1M_2 and B_1B_2 homozygous phenotypes). 400 samples for each value of dominance were used. Effect sizes span the boundaries of detection. Quantities in the simulation were based on the results of the analysis of the trait "DTP2," using Haley-Knott regression and a step size of 5 and a LOD threshold of 4.5. The simulations model a normally distributed trait, with QTL effect sizes ranging from 0 to 5, and a constant residual variance of 30 within each genotypic class, and assume no genotyping errors and no missing values. After detecting four QTL, all QTL were entered into a linear model in R/qtl. Obtained effect sizes for the four QTL ranged from LODs of 5 to 8, with a residual variance of about 28. Exploration with these numbers showed that effect sizes between 0 and 5 led to probabilities of detection ranging from about 0 to about 1.

Overlap with marine-freshwater divergent regions

The number of marine-freshwater divergent genomic regions that show evidence of repeated selection [the HMM or CSS signals of selection from (JONES *et al.* 2012)] within the 1.5 LOD interval of each QTL was determined. To test for enrichment of signals of selection within various groups of QTL, the mean number of overlaps of the QTL group was divided by the mean number of overlaps from 1000 simulations of random placement of signals of selection across the genome. P values were calculated by comparing the mean number of signal of selection-QTL overlaps to a null distribution of simulated placements of signals of selection. For determining the number of signals of selection overlapping the three trait clusters, the following coordinates were used: 2.34-28.56 Mb, 1.71-14.68 Mb, and 0-8.94 Mb for chromosomes 4, 20, and 21, respectively. These physical coordinates correspond to the genetic range on each chromosome that spans all of the clustered QTL shown in Figure 7, based upon markers flanking the 1.5-LOD interval listed in File S3. These coordinates were also used to identify putative

developmental regulatory genes within the trait clusters with Gene Ontology (GO) terms of "multicellular organismal development," "growth factor activity," or "regulation of transcription, DNA-dependent."

Files S2-S4

Available for download as Excel files at http://www.genetics.org/lookup/suppl/doi:10.1534/genetics.114.162420/-/DC1

File S2 Genotype and Phenotype data

All raw phenotype, adjusted phenotype (see Table S2) and genotype data used for QTL mapping. Raw genotypes were coded as follows: A and C are the marine grandparental alleles, B and D are the freshwater grandparental alleles. Genotypes of F2 fish were coded as follows: NA = missing, 1 = AC, 2 = BC, 3 = AD, 4 = BD, 5 = A = AC or AD, 6 = B = BC or BD, 7 = C = AC or BC, 8 = D = AD or BD, 10 = AD or BC.

File S3 Summary of all trait QTL

All detected significant QTL affecting skeletal traits are shown. QTL statistics are displayed in two ways: 1) allowing interpolated markers calculated every cM to be the peak markers or boundaries of the 1.5 LOD intervals or 2) allowing only real markers to be the peak markers or boundaries of the 1.5 LOD intervals. Mean phenotypes are displayed for Z scored phenotypes after size adjustment, sex adjustment, and log transformation, as necessary. For each QTL, one additive effect (half the difference between the two homozygous classes) and two dominance effects (difference between a heterozygous class and the mean of the two homozygous classes) is shown, as well as two dominance values (*d/a).* QTL in raker, opercle, median fin, and vertebrae classes that had expected directions of evolutionary change were determined to be concordant or antagonistic to the direction of evolutionary change.

File S4 Summary of principal component QTL

All detected significant QTL for the five largest principal components (PC1-5) are shown. QTL statistics are displayed in two ways: 1) allowing interpolated markers calculated every cM to be the peak markers or boundaries of the 1.5 LOD intervals or 2) allowing only real markers to be the peak markers or boundaries of the 1.5 LOD intervals.

Table S1 New microsatellites added to stickleback genetic linkage map

Stn marker	Nearby gene or marker	Forward primer sequence (5' to 3')	Reverse primer sequence (5' to 3')	BAC	Methods (see legend)	Accession # of BAC end sequence	Accession # of genetic marker
Stn338	***Dlx5/6***	CACCGCTAGTGTGTGTCTGC	CGCTCTCAAGACCACTCAGG		1		Pr031952730
Stn339	***Dlx1/2***	CAGCAATAGACACACACAGACG	CTGGGCTAAATATGATCCGTTC	14L21.SP6	2,3	KG777549	Pr031952731
Stn340	Stn207	CTAGAAGTCTGAAGAGCTCA	GCAATGATGAGGTCACCAG	75L11.SP6	2,3	KG777550	Pr031952732
Stn343	***Msx1***	TTACAATGGCTGGAGAGACG	CTCAGGCTATTTCTGAGACTCG	40L14.T7	2,3,4,5	KG777551	Pr031952733
Stn418*	EaccMgtg	TGCTGTCTTCAAGCCGTTTTC	GATAATAAGGACTCAAATAATTCAG	187B17.T7	2,5,6,7	CL648612	Pr031952734
Stn419^	Stn48	AGGAAGCTGCAGAGTTCAGG	TGACACCGACAGGCTTCC	49M10	2,3	KG777552	Pr031952735
Stn420	Stn292	CCCTGCTGTTGCACAATG	CTCAGCTGTTGGGAATTATGG	281G07.T7	2,3,5	KG777553	Pr031952736
Stn421	Stn222	CACTCCAGATGGAATCTCTGC	CCTCGACACACACAGATAAACC	168B20.T7	2,5,6	CL648236	Pr031952737
Stn422	*Bmp6*	CTGCCTCATATGGCATGAAG	CCCAGTTGTTGAGTTGGTTG	28D13.T7	2,5,6	CL642350	Pr031952738
Stn423	Stn422	CCTCCAGGACGAATTCAAAG	CTGCATCTCGGCTGTGTGG	258J06.T7	2,5,6,7	CL649886	Pr031952739
Stn424	*Zic1*	AGGTCTCGGTTCGATTACCA	TTGTGCGCTTGCATATGCAT		8		Pr031952740
Stn425	*Rnf32*	CGATTCAACCGACCCAACAC	ACACAGTCCAAACCGTCTCT		8		Pr031952741
Stn427	***Dlx3b***	ACACACACGCACAACACAGC	CCAGAGACGCAACGTGTAGG	72B08.SP6	2,3,4,5	KG777554	Pr031952742
Stn428	***Kit***	CCTGCGCAGAAATAGAGAGG	CGTATTCGGTAGCAGTCACC		8		Pr031952743
Stn429	***Edn1***	CACCCTTACAGGCGATTCAG	CATGTGTTGCATCATGCGTC		8		Pr031952744
Stn430	***Dlx3a***	CGGTCAGATGTGACGAGTG	CGTTGCTGATTCCTCTTGCG	69L16.SP6	2,3,4,5	KG777555	Pr031952745
Stn483	***Bmp6***	CCCGGTTTAAATCCTCATCC	AGGAGGTGATTGACAGCTCG		8		Pr031952746

For each marker, Stn number is listed, as well as nearby gene or genomic region. Markers that appear on the map (Fig. S1) as a gene have the gene name listed in bold. Markers that were discovered from sequence from marine BACs (CHORI 213 BAC library) have the BAC coordinate listed, and when microsatellite was found from BAC end sequence, that BAC end (T7 or SP6) is listed. For genotyping, all forward primers were 5' FAM labeled (Integrated DNA Technologies). In some cases, the first nucleotide of the forward primer was changed from G to C to prevent quenching of FAM. Methods used to identify new markers: 1= PCR amplicon sequencing, 2= BAC screening with overgoes, 3= BAC (end or internal) sequencing, 4= degenerate RT-PCR to find sequence for overgoes, 5= physical map information used (KINGSLEY *et al.* 2004), 6= publicly available BAC end sequences, 7= sequence homology with publicly available BAC end sequences, 8= genome assembly (JONES *et al.* 2012). Primer and overgo sequences used in marker discovery are listed in Supplemental Methods Text S1. *EaccMgtg was an AFLP linked to the plates locus (COLOSIMO *et al.* 2005). The sequence used to design Stn418 is highly repetitive in the stickleback genome and although this marker worked in this cross, it is not recommended. ^ For Stn419, BAC 49M10 was internally sequenced with Stn48 forward primer (PEICHEL *et al.* 2001).

References

COLOSIMO, P. F., K. E. HOSEMANN, S. BALABHADRA, G. VILLARREAL, JR., M. DICKSON *et al.*, 2005 Widespread parallel evolution in sticklebacks by repeated fixation of *Ectodysplasin* alleles. Science **307:** 1928-1933.

JONES, F. C., M. G. GRABHERR, Y. F. CHAN, P. RUSSELL, E. MAUCELI *et al.*, 2012 The genomic basis of adaptive evolution in threespine sticklebacks. Nature **484:** 55-61.

KINGSLEY, D. M., B. L. ZHU, K. OSOEGAWA, P. J. DE JONG, J. SCHEIN *et al.*, 2004 New genomic tools for molecular studies of evolutionary change in threespine sticklebacks. Behaviour **141:** 1331-1344.

PEICHEL, C. L., K. S. NERENG, K. A. OHGI, B. L. COLE, P. F. COLOSIMO *et al.*, 2001 The genetic architecture of divergence between threespine stickleback species. Nature **414:** 901-905.

Table S2 Trait descriptions and transformations

Trait	Description	Class	Model	Number of QTL
R1E	Row 1 epi raker number	raker	Raw	1
R2E	Row 2 epi raker number	raker	SL lm	1
R3E	Row 3 epi raker number	raker	Raw	1
R4E	Row 4 epi raker number	raker	Glm	0
R5E	Row 5 epi raker number	raker	Raw	0
R6E	Row 6 epi raker number	raker	Sex lm	1
R7E	Row 7 epi raker number	raker	Raw	0
R2J	Row 2 joint raker number	raker	SL lm	3
R4J	Row 4 joint raker number	raker	SL lm	1
R6J	Row 6 joint raker number	raker	Sex lm	2
R7J	Row 7 joint raker number	raker	Sex lm	0
R8J	Row 8 joint raker number	raker	Sex lm	0
R1C	Row 1 cerato raker number	raker	Glm	3
R2C	Row 2 cerato raker number	raker	Sex lm	2
R3C	Row 3 cerato raker number	raker	Glm	4
R4C	Row 4 cerato raker number	raker	Glm	4
R5C	Row 5 cerato raker number	raker	SL lm	2
R6C	Row 6 cerato raker number	raker	Glm	3
R7C	Row 7 cerato raker number	raker	Glm	1
R8C	Row 8 cerato raker number	raker	Sex lm	4
R9C	Row 9 cerato raker number	raker	SL lm	2
R1H	Row 1 hypo raker number	raker	Glm	0
R3H	Row 3 hypo raker number	raker	Raw	1
R5H	Row 5 hypo raker number	raker	SL lm	1
R7H	Row 7 hypo raker number	raker	Sex lm	1
E	Epi raker number	raker	Glm	1
J	Joint raker number	raker	Glm	4
C	Cerato raker number	raker	Glm	5
H	Hypo raker number	raker	Glm	6
R1	Row 1 raker number	raker	SL lm	5
R2	Row 2 raker number	raker	Sex lm	2
R3	Row 3 raker number	raker	Raw	5
R4	Row 4 raker number	raker	Sex lm	2
R5	Row 5 raker number	raker	Raw	2
R6	Row 6 raker number	raker	SL lm	2
R7	Row 7 raker number	raker	Glm	0
R8	Row 8 raker number	raker	Raw	1
BA1	Branchial arch 1 raker number	raker	Sex lm	6
BA2	Branchial arch 2 raker number	raker	Sex lm	6
BA3	Branchial arch 3 raker number	raker	Glm	4

BA4	Branchial arch 4 raker number	raker	SL lm	4
ODD	Odd row raker number	raker	Glm	5
EVEN	Even row raker number	raker	Sex lm	5
ALL	All raker number	raker	Glm	8
LSP	Lateral raker spacing	raker	SL lm	5
MISP	Middle raker spacing	raker	Glm	5
MESP	Medial raker spacing	raker	SL lm	1
DTP1	Dorsal toothplate 1 tooth number	teeth	Raw	6
DTP2	Dorsal toothplate 2 tooth number	teeth	Raw	7
VTP	Ventral toothplate tooth number	teeth	SL lm	5
PMT	Premaxilla tooth number	teeth	Glm	0
PMTR	Number of tooth rows on premaxilla	teeth	Glm	0
DTP1L	Dorsal toothplate 1 length	teeth	Glm	5
DTP1W	Dorsal toothplate 1 width	teeth	Glm	3
DTP2L	Dorsal toothplate 2 length	teeth	SL lm	6
DTP2W	Dorsal toothplate 2 width	teeth	Glm	5
VTPL	Ventral toothplate length	teeth	SL lm	3
VTPW	Ventral toothplate width	teeth	Glm	5
EB1L	Epibranchial 1 length	branchial	Glm	8
CB1L	Ceratobranchial 1 length	branchial	Glm	9
CB2L	Ceratobranchial 2 length	branchial	Glm	8
CB3L	Ceratobranchial 3 length	branchial	Glm	6
CB4L	Ceratobranchial 4 length	branchial	Glm	10
CB5L	Ceratobranchial 5 length	branchial	Glm	9
PML	Premaxilla length	jaw	Glm	9
PMW	Premaxilla width	jaw	Glm	2
PMH	Premaxilla height	jaw	Glm	5
DL	Dentary length	jaw	Glm	4
DH	Dentary height	jaw	Glm	4
AL	Articular length	jaw	Glm	7
AH	Articular height	jaw	Glm	3
IL1	In-lever 1 of articular length	jaw	Glm	3
IL2	In-lever 2 of articular length	jaw	Glm	3
FW	Frontal width	skull	Glm	7
SOL	Supraoccipital crest length	skull	SL lm	2
SOW	Supraoccipital crest width	skull	SL lm	4
SOA	Supraoccipital crest area	skull	SL lm	6
OPL	Opercle length	opercle	Glm	3
OPW	Opercle width	opercle	Glm	4
OPN	Opercle neck width	opercle	Sex lm	2
DS1L	Dorsal spine 1 length	median fin	SL lm	8
DS2L	Dorsal spine 2 length	median fin	Glm	9
DS3L	Dorsal spine 3 length	median fin	Glm	5

ASL	Anal spine length	median fin	Glm	3
SR	Serration number on dorsal spine 2	median fin	Glm	2
SRA	Serration area on dorsal spine 2	median fin	Glm	2
SPA	Dorsal spine 2 area	median fin	SL lm	2
SDS2A	Smoothened dorsal spine 2 area (SPA-SRA)	median fin	SL lm	1
DFR	Dorsal fin ray number	median fin	Sex lm	1
AFR	Anal fin ray number	median fin	Glm	1
PD	Predorsal pterygiophore number	median fin	Sex lm	0
PE	Non-ray-bearing postdorsal pterygiophore number	median fin	Raw	1
PN	Non-ray-bearing postanal pterygiophore number	median fin	Raw	1
TPDP	Total postdorsal pterygiophore number	median fin	Sex lm	1
TAP	Total postanal pterygiophore number	median fin	Sex lm	2
TDP	Total dorsal pterygiophore number	median fin	Sex lm	1
PD3	Third predorsal pterygiophore position	vertebrae	Raw	2
PD4	Fourth predorsal pterygiophore position	vertebrae	Raw	0
PD5	Fifth predorsal pterygiophore position	vertebrae	Sex lm	0
FDP	First postdorsal pterygiophore position	vertebrae	Sex lm	0
LDP	Last postdorsal pterygiophore position	vertebrae	Raw	4
FAP	First postanal pterygiophore position	vertebrae	Sex lm	0
LAP	Last postanal pterygiophore position	vertebrae	Raw	5
FHS	First hemal spine position	vertebrae	Sex lm	0
LDFR	Last dorsal fin ray position	vertebrae	SL lm	0
LAFR	Last anal fin ray position	vertebrae	Raw	3
VN	Vertebrae number	vertebrae	Sex lm	2
AVN	Abdominal vertebrae number	vertebrae	Sex lm	0
CVN	Caudal vertebrae number	vertebrae	Sex lm	1
VR	Vertebrae ratio (AVN/CVN)	vertebrae	Sex lm	0

Depending on the relationship of phenotype with standard length (SL) and sex, the phenotype used for QTL mapping was unadjusted (raw), residuals from a SL regression (SL lm), residuals from one-way ANOVA using sex as a factor (Sex lm), or residuals from a SL+Sex General Linear Model ANOVA (Glm). Units are meristic counts for number traits, millimeters for linear measurements, millimeters^2 for area traits, vertebrae number for vertebral position traits (see Supplemental Methods Text S1) or unitless for VR. For 92 of 110 traits, at least one QTL was detected.

Table S3 Sexually dimorphic traits

Trait	P-value	Male		Female	
		Mean +/- SE	n	Mean +/- SE	n
R4E*	7.03E-05	0.861 +/- 0.043	168	0.637 +/- 0.038	188
R6E	3.25E-05	1.70 +/- 0.052	168	1.43 +/- 0.041	187
R6J	1.18E-05	2.52 +/- 0.046	168	2.79 +/- 0.040	188
R7J	5.99E-03	1.36 +/- 0.054	168	1.56 +/- 0.051	187
R8J	1.09E-02	1.79 +/- 0.049	168	1.96 +/- 0.045	188
R1C*	3.02E-03	11.4 +/- 0.064	168	11.1 +/- 0.057	188
R2C	1.21E-05	11.4 +/- 0.061	168	11.1 +/- 0.055	188
R3C*	1.30E-02	11.0 +/- 0.069	168	10.8 +/- 0.059	188
R4C*	4.96E-09	11.3 +/- 0.053	168	10.9 +/- 0.043	188
R6C*	2.98E-02	11.8 +/- 0.063	168	11.6 +/- 0.053	188
R7C*	6.69E-10	13.0 +/- 0.065	168	12.5 +/- 0.052	188
R8C	1.47E-03	11.0 +/- 0.058	168	10.8 +/- 0.057	188
R1H*	1.92E-02	2.50 +/- 0.045	167	2.64 +/- 0.037	187
R7H	1.83E-07	0.339 +/- 0.037	168	0.612 +/- 0.036	188
E*	2.98E-03	13.4 +/- 0.15	168	12.8 +/- 0.13	186
J*	1.09E-05	11.4 +/- 0.14	168	12.2 +/- 0.12	187
C*	1.34E-06	105 +/- 0.38	168	103 +/- 0.32	188
H*	1.54E-03	8.49 +/- 0.085	167	8.84 +/- 0.070	187
R2	1.48E-03	14.8 +/- 0.072	168	14.5 +/- 0.066	188
R4	1.68E-11	15.1 +/- 0.065	168	14.5 +/- 0.055	188
R7*	3.05E-02	16.0 +/- 0.070	168	15.8 +/- 0.067	187
BA1	2.69E-02	34.5 +/- 0.15	167	34.0 +/- 0.13	186
BA2	1.95E-05	30.5 +/- 0.12	168	29.8 +/- 0.10	188
BA3*	4.62E-02	31.7 +/- 0.12	168	31.4 +/- 0.10	187
ODD*	4.55E-02	79.6 +/- 0.27	167	78.9 +/- 0.24	185
EVEN	6.85E-05	58.8 +/- 0.21	168	57.7 +/- 0.18	187
ALL*	1.24E-03	138 +/- 0.46	167	136 +/- 0.39	185
MISP*	1.85E-02	0.291 +/- 0.0017	167	0.286 +/- 0.0015	188
PMT*	1.23E-35	26.9 +/- 0.43	172	20.1 +/- 0.29	195
PMTR*	1.34E-33	2.64 +/- 0.034	172	2.11 +/- 0.024	195
DTP1L*^	6.49E-04	0.891 +/- 0.0039	168	0.872 +/- 0.0043	187
DTP1W*	1.91E-10	0.373 +/- 0.0026	168	0.397 +/- 0.0028	188
DTP2W*	1.01E-08	0.648 +/- 0.0033	168	0.674 +/- 0.0031	188
VTPW*^	8.16E-05	0.436 +/- 0.0038	168	0.417 +/- 0.0030	188
EB1L*^	3.28E-19	1.37 +/- 0.0069	168	1.28 +/- 0.0062	188
CB1L*^	1.14E-18	3.12 +/- 0.0083	168	3.01 +/- 0.0084	188
CB2L*^	8.56E-18	2.91 +/- 0.0080	168	2.80 +/- 0.0080	188
CB3L*	4.11E-14	2.71 +/- 0.0074	168	2.63 +/- 0.0074	188
CB4L*^	2.01E-13	2.65 +/- 0.0075	168	2.57 +/- 0.0073	188

CB5L*^	4.07E-07	2.55 +/- 0.0071	168	2.50 +/- 0.0072	188
PML*^	5.16E-63	2.66 +/- 0.011	172	2.39 +/- 0.0085	194
PMW*^	2.30E-31	0.361 +/- 0.0030	172	0.310 +/- 0.0027	194
PMH*	4.29E-14	2.48 +/- 0.0083	172	2.39 +/- 0.0085	195
DL*	5.13E-24	1.90 +/- 0.0094	165	1.77 +/- 0.0085	186
DH*	2.17E-31	1.39 +/- 0.0063	166	1.28 +/- 0.0063	188
AL*^	2.92E-45	2.52 +/- 0.011	169	2.29 +/- 0.0097	189
AH*^	7.86E-20	0.965 +/- 0.0077	168	0.867 +/- 0.0068	187
IL1*^	2.21E-02	0.859 +/- 0.0061	168	0.840 +/- 0.0053	188
IL2*	3.93E-21	1.41 +/- 0.0069	168	1.31 +/- 0.0066	187
FW*	3.33E-09	2.52 +/- 0.010	172	2.43 +/- 0.010	195
OPL*^	6.31E-21	4.06 +/- 0.013	171	3.88 +/- 0.012	194
OPW*^	3.53E-35	4.09 +/- 0.014	170	3.84 +/- 0.012	192
OPN	1.93E-11	0.288 +/- 0.0072	171	0.236 +/- 0.0031	195
DS2L*^	7.55E-03	3.80 +/- 0.033	167	3.92 +/- 0.029	195
DS3L*^	3.84E-17	0.958 +/- 0.012	168	1.12 +/- 0.015	194
ASL*	5.29E-27	0.994 +/- 0.015	150	1.22 +/- 0.013	178
SR*	7.55E-06	4.55 +/- 0.21	169	3.29 +/- 0.19	193
SRA*	2.58E-14	0.0613 +/- 0.0036	167	0.0292 +/- 0.0022	192
DFR	2.06E-02	10.9 +/- 0.047	168	10.7 +/- 0.042	189
AFR*	1.70E-08	7.88 +/- 0.046	168	7.53 +/- 0.043	189
PD	6.87E-03	6.02 +/- 0.022	169	6.11 +/- 0.023	190
TPDP	9.14E-05	13.8 +/- 0.046	168	13.6 +/- 0.044	189
TAP	7.82E-10	10.9 +/- 0.050	168	10.5 +/- 0.043	189
TDP	1.89E-02	19.9 +/- 0.050	168	19.7 +/- 0.048	189
PD5	9.09E-06	9.91 +/- 0.021	170	10.1 +/- 0.022	195
FDP	2.92E-08	11.7 +/- 0.034	170	11.9 +/- 0.023	193
FAP	2.09E-19	15.6 +/- 0.038	167	16.0 +/- 0.019	193
FHS	1.27E-19	15.5 +/- 0.038	170	16.0 +/- 0.021	194
VN	1.77E-11	31.5 +/- 0.039	162	31.2 +/- 0.031	190
AVN	1.27E-19	14.5 +/- 0.038	170	15.0 +/- 0.021	194
CVN	4.69E-31	17.0 +/- 0.048	162	16.2 +/- 0.035	189
VR	1.78E-31	0.859 +/- 0.0042	162	0.922 +/- 0.0027	189

Mean and standard error of phenotypes within males and females are shown for traits that were significantly sexually dimorphic by two-tailed Student's t test. *Trait was corrected for body size and standardized to 40 mm length. ^Trait was log-adjusted.

Table S4 Summary of filtered QTL

Trait	Class	LG	Marker	LOD	PVE	Mean +/- Standard Error (n)			
						M_1M_2	M_1B_1	M_2B_2	B_1B_2
R3C	raker	1	Stn2	4.7	3.8	10.8 +/- 0.085	10.85 +/- 0.086	10.85 +/- 0.084	10.59 +/- 0.1
BA2	raker	1	Stn5	10.7	7.5	30.4 +/- 0.15	29.9 +/- 0.13	29.8 +/- 0.13	29.2 +/- 0.19
R3E	raker	2	Stn17	5.1	6.4	1.387 +/- 0.057	1.63 +/- 0.061	1.521 +/- 0.056	1.765 +/- 0.05
E	raker	4	Stn38	8.6	10.6	11.83 +/- 0.2	12.78 +/- 0.17	13.06 +/- 0.17	13.55 +/- 0.17
LSP	raker	4	Stn47	27.7	22.6	0.254 +/- 0.0019	0.264 +/- 0.0025	0.2721 +/- 0.0026	0.2885 +/- 0.0024
MISP	raker	6	Stn62	4.9	3.4	0.2921 +/- 0.0025	0.282 +/- 0.0025	0.2841 +/- 0.0021	0.2851 +/- 0.0019
H	raker	7	Stn258	6.1	5.7	9.113 +/- 0.097	8.975 +/- 0.11	8.682 +/- 0.11	8.555 +/- 0.11
R1C	raker	7	Stn75	7.8	7.0	11.39 +/- 0.082	11.07 +/- 0.078	11.23 +/- 0.083	10.8 +/- 0.085
R8C	raker	8	Stn300	5.3	5.5	10.71 +/- 0.081	10.68 +/- 0.081	10.82 +/- 0.074	10.98 +/- 0.087
H	raker	8	Stn95	5.0	4.6	8.679 +/- 0.11	9.03 +/- 0.11	8.684 +/- 0.11	8.965 +/- 0.11
R6J	raker	10	Stn124	5.6	6.4	2.968 +/- 0.059	2.704 +/- 0.058	2.879 +/- 0.062	2.632 +/- 0.056
LSP	raker	11	Stn244	6.0	4.2	0.278 +/- 0.003	0.2694 +/- 0.003	0.2685 +/- 0.002	0.2656 +/- 0.0031
BA2	raker	12	Nemo	4.2	2.8	30.06 +/- 0.16	29.91 +/- 0.17	29.77 +/- 0.16	29.67 +/- 0.14
MISP	raker	13	Stn155	5.2	3.6	0.2873 +/- 0.0018	0.2837 +/- 0.0022	0.2887 +/- 0.0024	0.2828 +/- 0.0022
EVEN	raker	14	Stn166	4.5	3.4	57.11 +/- 0.28	57.6 +/- 0.28	57.66 +/- 0.28	58.28 +/- 0.27
R9C	raker	15	Stn230	7.3	7.8	12.98 +/- 0.081	12.82 +/- 0.083	13.05 +/- 0.089	12.42 +/- 0.079
BA1	raker	16	Stn176	6.6	5.0	33.75 +/- 0.21	34.6 +/- 0.19	33.55 +/- 0.18	34.3 +/- 0.19
H	raker	17	Stn323	5.5	5.1	9.067 +/- 0.11	9.017 +/- 0.1	8.905 +/- 0.11	8.419 +/- 0.11
ALL	raker	17	Stn205	8.4	5.1	137.7 +/- 0.49	137.5 +/- 0.54	136 +/- 0.69	134.4 +/- 0.61
ALL	raker	18	Stn305	4.6	2.8	137.6 +/- 0.9	135.1 +/- 0.63	136.6 +/- 0.49	136.7 +/- 0.54
C	raker	20	Stn215	32.9	25.3	105.6 +/- 0.37	103.4 +/- 0.44	101.5 +/- 0.39	98.88 +/- 0.52
R8C	raker	20	Gac1125	9.0	9.5	11.03 +/- 0.065	10.9 +/- 0.083	10.58 +/- 0.083	10.56 +/- 0.087
H	raker	21	Stn223	4.6	4.2	9.128 +/- 0.1	8.858 +/- 0.11	8.676 +/- 0.11	8.682 +/- 0.11
VTPW	teeth	1	Stn272	6.3	4.8	0.4276 +/- 0.0059	0.4197 +/- 0.0038	0.4191 +/- 0.0044	0.398 +/- 0.0045
DTP2L	teeth	1	Stn13	4.5	3.7	1.493 +/- 0.0077	1.48 +/- 0.0077	1.469 +/- 0.0074	1.471 +/- 0.0074
DTP2L	teeth	2	Stn259	7.8	6.7	1.507 +/- 0.0079	1.478 +/- 0.008	1.47 +/- 0.0068	1.463 +/- 0.0071
VTPW	teeth	2	Stn24	6.5	5.0	0.4169 +/- 0.0046	0.4202 +/- 0.0053	0.4082 +/- 0.004	0.4245 +/- 0.0053

DTP2	teeth	4	Eda	34.9	24.2	53.96 +/- 0.68	49.06 +/- 0.66	47.3 +/- 0.66	44.68 +/- 0.61
DTP1	teeth	7	Stn72	6.9	5.1	15.63 +/- 0.29	16.59 +/- 0.34	16.27 +/- 0.29	17.53 +/- 0.35
DTP2L	teeth	7	Stn75	15.2	13.7	1.444 +/- 0.0071	1.47 +/- 0.0062	1.488 +/- 0.0079	1.515 +/- 0.0076
DTP2	teeth	8	Stn300	7.1	4.1	50.06 +/- 0.67	49.11 +/- 0.71	47.8 +/- 0.69	47.67 +/- 0.89
DTP2W	teeth	8	Stn95	5.1	4.2	0.662 +/- 0.0054	0.6832 +/- 0.0037	0.6658 +/- 0.004	0.6852 +/- 0.0048
DTP1L	teeth	9	Stn102	5.6	4.7	0.8897 +/- 0.0056	0.8756 +/- 0.0055	0.866 +/- 0.0057	0.8527 +/- 0.0058
DTP2	teeth	10	Stn211	12.7	7.6	49.97 +/- 0.61	49.28 +/- 0.84	49.41 +/- 0.88	46.03 +/- 0.58
DTP1	teeth	11	Dlx3a	6.1	4.5	15.82 +/- 0.32	15.67 +/- 0.29	16.63 +/- 0.29	17.43 +/- 0.35
DTP2W	teeth	12	Stn232	5.4	4.4	0.6858 +/- 0.0042	0.6727 +/- 0.0042	0.6802 +/- 0.0053	0.6631 +/- 0.0042
DTP1W	teeth	12	Stn142	4.7	5.2	0.4122 +/- 0.0043	0.3963 +/- 0.0033	0.3958 +/- 0.0037	0.3915 +/- 0.0039
VTP	teeth	13	Stn153	5.5	3.9	45.24 +/- 0.7	47.98 +/- 0.81	46.41 +/- 0.8	48.34 +/- 0.7
DTP2W	teeth	14	Stn198	7.0	5.8	0.6828 +/- 0.0047	0.6637 +/- 0.0038	0.6706 +/- 0.0047	0.685 +/- 0.0047
DTP1L	teeth	14	Stn237	6.6	5.6	0.8505 +/- 0.0051	0.8798 +/- 0.0059	0.8716 +/- 0.0062	0.882 +/- 0.0055
DTP1L	teeth	16	Stn178	7.4	6.4	0.8617 +/- 0.0065	0.8639 +/- 0.0059	0.873 +/- 0.0051	0.8844 +/- 0.0058
DTP2	teeth	20	Stn215	12.8	7.6	50.99 +/- 0.61	49.35 +/- 0.74	48.14 +/- 0.7	44.82 +/- 0.8
VTP	teeth	21	Stn422	31.0	26.2	42.28 +/- 0.56	46.48 +/- 0.69	46.93 +/- 0.58	52.48 +/- 0.76
CB2L	branchial	1	Stn248	6.2	4.2	2.821 +/- 0.012	2.804 +/- 0.011	2.789 +/- 0.011	2.786 +/- 0.011
EB1L	branchial	2	Stn21	11.6	6.7	1.308 +/- 0.01	1.288 +/- 0.0091	1.269 +/- 0.0085	1.257 +/- 0.0083
CB1L	branchial	2	Stn268	14.9	10.4	3.056 +/- 0.011	3.019 +/- 0.013	3.007 +/- 0.01	2.973 +/- 0.012
CB4L	branchial	4	Stn45	29.3	19.1	2.514 +/- 0.0084	2.555 +/- 0.01	2.574 +/- 0.01	2.64 +/- 0.0087
CB5L	branchial	5	Stn52	8.6	5.9	2.46 +/- 0.01	2.49 +/- 0.01	2.5 +/- 0.01	2.533 +/- 0.0087
EB1L	branchial	5	Stn312	6.6	3.7	1.254 +/- 0.011	1.269 +/- 0.0087	1.281 +/- 0.0077	1.303 +/- 0.0089
EB1L	branchial	7	Stn71	7.4	4.2	1.262 +/- 0.0085	1.265 +/- 0.0089	1.276 +/- 0.0091	1.312 +/- 0.0092
EB1L	branchial	8	Stn239	9.6	5.5	1.244 +/- 0.0083	1.3 +/- 0.0092	1.267 +/- 0.0092	1.296 +/- 0.0088
CB4L	branchial	10	Edn1	6.0	3.3	2.551 +/- 0.0088	2.547 +/- 0.012	2.583 +/- 0.0096	2.607 +/- 0.011
CB4L	branchial	12	Stn287	6.2	3.5	2.54 +/- 0.01	2.574 +/- 0.0095	2.572 +/- 0.011	2.6 +/- 0.01
EB1L	branchial	14	Stn163	7.1	4.0	1.259 +/- 0.0075	1.283 +/- 0.0093	1.266 +/- 0.0096	1.303 +/- 0.0096
CB1L	branchial	15	Stn173	7.4	4.9	3.04 +/- 0.014	3.027 +/- 0.0094	2.998 +/- 0.011	2.973 +/- 0.013
CB4L	branchial	16	Edar	6.9	3.9	2.558 +/- 0.011	2.558 +/- 0.011	2.597 +/- 0.009	2.574 +/- 0.011
CB2L	branchial	17	Stn325	7.1	4.9	2.773 +/- 0.012	2.811 +/- 0.0097	2.783 +/- 0.013	2.829 +/- 0.011
CB5L	branchial	18	Stn280	9.8	6.7	2.454 +/- 0.011	2.508 +/- 0.011	2.501 +/- 0.0083	2.517 +/- 0.0097

EB1L	branchial	21	Stn219	24.4	15.5	1.231 +/- 0.0079	1.273 +/- 0.009	1.289 +/- 0.0081	1.322 +/- 0.0088
PML	jaw	2	Stn24	5.3	3.7	2.39 +/- 0.013	2.405 +/- 0.014	2.361 +/- 0.012	2.37 +/- 0.015
PML	jaw	3	Stn31	5.2	3.7	2.344 +/- 0.012	2.405 +/- 0.015	2.363 +/- 0.012	2.415 +/- 0.014
IL2	jaw	4	Stn45	17.9	16.9	1.264 +/- 0.0082	1.297 +/- 0.008	1.302 +/- 0.009	1.366 +/- 0.0091
PML	jaw	5	Stn52	8.3	6.0	2.333 +/- 0.013	2.403 +/- 0.014	2.389 +/- 0.013	2.396 +/- 0.013
IL2	jaw	7	Stn75	13.1	11.9	1.267 +/- 0.0084	1.318 +/- 0.0085	1.305 +/- 0.0091	1.351 +/- 0.0099
PMW	jaw	7	Stn257	7.4	8.3	0.2965 +/- 0.0039	0.3029 +/- 0.004	0.3133 +/- 0.0042	0.3222 +/- 0.0035
AL	jaw	9	Stn102	8.0	5.6	2.329 +/- 0.013	2.304 +/- 0.014	2.289 +/- 0.014	2.22 +/- 0.013
PMH	jaw	11	Stn224	7.8	6.9	2.427 +/- 0.012	2.387 +/- 0.012	2.37 +/- 0.011	2.355 +/- 0.011
DH	jaw	12	Stn318	6.8	6.9	1.313 +/- 0.0085	1.279 +/- 0.0078	1.283 +/- 0.0096	1.249 +/- 0.0083
PMH	jaw	14	Stn331	5.9	5.2	2.345 +/- 0.013	2.399 +/- 0.011	2.372 +/- 0.012	2.419 +/- 0.01
AL	jaw	16	Dlx1/2	6.1	4.3	2.267 +/- 0.014	2.26 +/- 0.015	2.299 +/- 0.012	2.312 +/- 0.015
DL	jaw	17	Stn325	7.2	7.5	1.729 +/- 0.014	1.743 +/- 0.011	1.771 +/- 0.012	1.802 +/- 0.012
PML	jaw	19	Stn194	7.6	5.4	2.358 +/- 0.012	2.398 +/- 0.013	2.338 +/- 0.012	2.417 +/- 0.014
PMH	jaw	20	Stn216	5.2	4.5	2.408 +/- 0.011	2.396 +/- 0.012	2.373 +/- 0.012	2.34 +/- 0.012
PMH	jaw	21	Stn422	13.4	12.3	2.322 +/- 0.011	2.386 +/- 0.011	2.406 +/- 0.012	2.424 +/- 0.011
SOA	skull	1	Stn272	17.7	10.5	313.6 +/- 13	278.2 +/- 9.5	250.9 +/- 11	215.9 +/- 11
SOL	skull	4	Stn253	4.9	5.6	1.272 +/- 0.012	1.304 +/- 0.013	1.297 +/- 0.012	1.354 +/- 0.012
SOA	skull	6	Stn279	8.4	4.7	242.8 +/- 12	290.1 +/- 13	239.8 +/- 9.9	293.2 +/- 11
FW	skull	7	Stn72	6.8	5.4	2.4 +/- 0.014	2.387 +/- 0.015	2.453 +/- 0.012	2.474 +/- 0.016
SOA	skull	8	Stn88	6.3	3.5	289.3 +/- 9.9	269.6 +/- 10	267.5 +/- 12	234.2 +/- 13
SOL	skull	12	Stn318	7.8	9.0	1.253 +/- 0.013	1.298 +/- 0.012	1.339 +/- 0.013	1.34 +/- 0.011
SOA	skull	13	Stn156	8.3	4.7	298.9 +/- 12	268.9 +/- 11	264.3 +/- 12	236.7 +/- 10
SOA	skull	14	Stn167	6.2	3.4	265.8 +/- 11	258.9 +/- 10	254.5 +/- 13	282.9 +/- 11
FW	skull	15	Stn230	7.0	5.6	2.465 +/- 0.015	2.408 +/- 0.014	2.436 +/- 0.015	2.41 +/- 0.012
FW	skull	18	Stn280	4.8	3.8	2.4 +/- 0.014	2.414 +/- 0.015	2.435 +/- 0.014	2.457 +/- 0.014
SOA	skull	20	Stn216	43.0	30.4	340.2 +/- 11	257.6 +/- 9.4	251.1 +/- 9.6	183.2 +/- 7.2
FW	skull	21	Stn223	6.2	4.9	2.457 +/- 0.014	2.4 +/- 0.014	2.457 +/- 0.016	2.4 +/- 0.013
OPL	opercle	1	Stn272	11.4	10.9	3.928 +/- 0.019	3.919 +/- 0.015	3.858 +/- 0.017	3.794 +/- 0.017
OPW	opercle	2	Stn297	7.3	7.5	3.879 +/- 0.02	3.869 +/- 0.018	3.829 +/- 0.017	3.772 +/- 0.017
OPL	opercle	7	Stn79	11.6	11.1	3.797 +/- 0.016	3.893 +/- 0.017	3.897 +/- 0.019	3.942 +/- 0.016

OPW	opercle	7	Stn81	5.3	5.4	3.81 +/- 0.018	3.842 +/- 0.019	3.79 +/- 0.017	3.888 +/- 0.018
OPL	opercle	12	Stn275	9.6	9.1	3.818 +/- 0.017	3.839 +/- 0.016	3.915 +/- 0.018	3.929 +/- 0.017
OPW	opercle	17	Stn231	6.8	7.0	3.8 +/- 0.018	3.808 +/- 0.016	3.84 +/- 0.021	3.887 +/- 0.018
OPN	opercle	18	Stn196	8.5	9.2	0.2704 +/- 0.008	0.2063 +/- 0.0073	0.2229 +/- 0.0063	0.2364 +/- 0.0067
PE	median fin	1	Stn248	4.5	5.5	3.023 +/- 0.062	2.943 +/- 0.05	2.911 +/- 0.07	2.615 +/- 0.064
DS2L	median fin	2	Stn21	7.0	3.9	3.982 +/- 0.05	3.892 +/- 0.046	4.001 +/- 0.045	3.841 +/- 0.035
DS1L	median fin	3	Stn33	6.1	3.8	3.182 +/- 0.054	3.122 +/- 0.047	3.182 +/- 0.039	3.013 +/- 0.052
DS2L	median fin	4	Eda	51.1	38.2	4.302 +/- 0.042	3.96 +/- 0.033	3.751 +/- 0.038	3.685 +/- 0.032
TAP	median fin	4	Stn420	9.7	11.0	10.79 +/- 0.059	10.47 +/- 0.061	10.51 +/- 0.063	10.2 +/- 0.064
DS2L	median fin	5	Stn326	4.8	2.6	3.959 +/- 0.049	3.886 +/- 0.043	3.96 +/- 0.038	3.869 +/- 0.045
DS1L	median fin	7	Stn76	7.1	4.5	3.195 +/- 0.046	3.143 +/- 0.051	3.125 +/- 0.045	3.015 +/- 0.052
DS1L	median fin	8	Stn92	6.3	4.0	3.226 +/- 0.052	3.164 +/- 0.05	3.077 +/- 0.038	3.034 +/- 0.048
DS2L	median fin	9	Stn102	12.2	7.0	4.067 +/- 0.047	3.89 +/- 0.046	3.922 +/- 0.038	3.8 +/- 0.038
SRA	median fin	10	Stn121	6.0	6.7	0.01785 +/- 0.0035	0.02191 +/- 0.0037	0.03213 +/- 0.0049	0.04105 +/- 0.0038
DS2L	median fin	11	Stn224	4.5	2.5	3.845 +/- 0.04	3.887 +/- 0.045	3.915 +/- 0.042	4.018 +/- 0.044
DS3L	median fin	13	Stn155	5.5	4.6	1.127 +/- 0.02	1.15 +/- 0.016	1.09 +/- 0.018	1.121 +/- 0.02
DS2L	median fin	16	Stn299	8.0	4.5	4.059 +/- 0.051	3.906 +/- 0.045	3.902 +/- 0.038	3.815 +/- 0.036
ASL	median fin	17	Stn286	5.7	5.5	1.158 +/- 0.018	1.251 +/- 0.019	1.237 +/- 0.022	1.262 +/- 0.017
DS1L	median fin	18	Stn196	7.5	4.8	3.247 +/- 0.049	3.085 +/- 0.047	3.134 +/- 0.042	3.028 +/- 0.05
SRA	median fin	20	Stn212	7.9	9.0	0.04322 +/- 0.004	0.03082 +/- 0.0036	0.02228 +/- 0.0041	0.01077 +/- 0.0037
DS3L	median fin	21	Stn421	7.9	6.7	1.175 +/- 0.019	1.13 +/- 0.018	1.131 +/- 0.02	1.054 +/- 0.016
LAP	vertebrae	1	Stn240	13.1	10.9	25.68 +/- 0.05	25.49 +/- 0.049	25.33 +/- 0.056	25.21 +/- 0.051
LAP	vertebrae	4	Stn419	10.4	8.5	25.61 +/- 0.055	25.48 +/- 0.053	25.46 +/- 0.057	25.21 +/- 0.044
CVN	vertebrae	5	Stn58	5.0	6.4	16.32 +/- 0.062	16.43 +/- 0.062	16.12 +/- 0.059	16.13 +/- 0.042
LAFR	vertebrae	8	Stn87	5.9	14.9	22.55 +/- 0.15	22.33 +/- 0.11	22 +/- 0.14	22.52 +/- 0.085
LAP	vertebrae	10	Stn120	5.5	4.4	25.4 +/- 0.056	25.38 +/- 0.055	25.34 +/- 0.055	25.58 +/- 0.049
LAFR	vertebrae	15	Stn170	4.3	10.5	22.61 +/- 0.12	22.26 +/- 0.11	22.57 +/- 0.12	22.11 +/- 0.12
LAP	vertebrae	20	Stn340	8.3	6.7	25.55 +/- 0.05	25.37 +/- 0.052	25.52 +/- 0.055	25.25 +/- 0.057
LAP	vertebrae	21	Stn223	14.6	12.3	25.62 +/- 0.048	25.33 +/- 0.055	25.53 +/- 0.056	25.24 +/- 0.05

Only the non-overlapping QTL with highest LOD score within each trait class are shown. Phenotypes are presented as phenotype of a fish of 40 mm SL, with residuals added to each genotypic class (M_1M_2 is homozygous marine, B_1B_2 homozygous benthic, and MB classes the heterozygotes). For traits that were only size corrected, the linear regression equation was used, for traits both size and sex corrected, the GLM equation was used.

Table S5 Regional or global QTL controlling serially homologous skeletal elements

Category of homologous skeletal elements	Number and description of anatomical domains	Regional QTL (controlling subset of domains)	Global QTL (controlling all domains)
Gill raker number	25 domains in 9 anterior/posterior and 4 dorsal/ventral regions	10	0
Pharyngeal tooth number	2 dorsal, 1 ventral toothplate	4	4
Branchial bone length	1 dorsal, 5 ventral bones	10	4
Jaw size	1 dorsal, 1 ventral bone	7	5
Spine length	3 dorsal, 1 anal spine	13	1
Total	--	44	14

For each set of likely serially homologous skeletal elements, QTL controlling these elements were classified as controlling only a subset of the domains (anatomically regional) or controlling all the domains (global). Most QTL are anatomically regional, and this trend holds broadly across different trait classes.

Table S6 Dominance of QTL by phenotypic class

Class	Under-dominant	Recessive	Partially recessive	Additive	Partially dominant	Dominant	Over-dominant
raker	0.09	0.15	0.26	0.17	0.15	0.04	0.13
teeth	0.08	0.05	0.20	0.35	0.30	0.00	0.02
branchial	0.03	0.16	0.09	0.41	0.25	0.03	0.03
jaw	0.03	0.10	0.27	0.17	0.33	0.07	0.03
skull	0.04	0.00	0.25	0.50	0.12	0.08	0.00
opercle	0.07	0.21	0.21	0.21	0.14	0.00	0.14
median fin	0.09	0.12	0.24	0.29	0.15	0.06	0.06
vertebrae	0.06	0.12	0.31	0.06	0.19	0.12	0.12
gain	0.07	0.16	0.17	0.29	0.23	0.05	0.04
loss	0.06	0.07	0.27	0.27	0.20	0.05	0.08
all	0.06	0.11	0.22	0.28	0.21	0.05	0.06

Dominance (*d/a*) ranges for different dominance classes follow cut-offs of (BURKE *et al.* 2002): < -1.25 for underdominant, -1.25 to -0.75 for recessive, -0.75 to -0.25 for partially recessive, -0.25 to 0.25 for additive, 0.25-0.75 for partially dominant, 0.75-1.25 for dominant and >1.25 for overdominant. For each dominance class, the proportion of filtered QTL that have dominance values within that range are listed. A tendency towards additive and partially additive QTL is seen broadly across trait classes. Constructive (gain) QTL and regressive (loss) QTL also show a trend towards additivity.

Table S7 Trait clustering *P* values

Chromosome	All QTL			Large effect QTL		
	Genetic	Physical	Gene number	Genetic	Physical	Gene number
1	0.59	0.39	0.33	0.16	0.09	0.07
2	0.78	0.58	0.36	0.90	0.83	0.75
3	0.99	0.99	1.00	1.00	1.00	1.00
4	0.22	0.50	0.37	**0.00**	**0.01**	**0.00**
5	0.97	0.64	0.80	1.00	1.00	1.00
6	0.98	1.00	0.99	1.00	1.00	1.00
7	0.41	0.37	0.36	0.27	0.27	0.27
8	0.90	0.41	0.38	0.94	0.77	0.76
9	1.00	0.99	0.99	0.81	0.78	0.80
10	0.76	0.56	0.62	0.76	0.70	0.73
11	0.97	0.85	0.95	1.00	1.00	1.00
12	0.57	0.38	0.49	0.80	0.75	0.81
13	0.81	0.93	0.93	1.00	1.00	1.00
14	0.80	0.53	0.55	1.00	1.00	1.00
15	0.08	0.83	0.83	1.00	1.00	1.00
16	0.51	0.68	0.60	1.00	1.00	1.00
17	0.78	0.49	0.50	1.00	1.00	1.00
18	0.75	0.59	0.56	0.75	0.71	0.70
20	0.09	0.43	0.42	**0.03**	0.14	0.14
21	**0.00**	**0.02**	**0.01**	**0.00**	**0.01**	**0.00**

P values for enrichment of QTL on each chromosome for all QTL or large effect QTL were calculated by comparing the actual number of QTL per chromosome to the distribution from 1000 simulated placements of QTL. Simulations were ran assuming QTL were randomly placed in proportion to the 1) the genetic length of the chromosome, 2) the physical length of the chromosome, or 3) the number of Ensembl-predicted genes on the chromosome. *P* values less than 0.05 are in bold. Relative to simulated QTL placed in proportion to the genetic length of each chromosome, large effect QTL (the top quartile of QTL by LOD) are significantly enriched on chromosomes 4, 20, and 21.

LITERATURE CITED

AHN, D. G., and G. GIBSON, 1999 Axial variation in the three-spine stickleback: genetic and environmental factors. Evol Dev **1:** 100-112.

ALBERT, A. Y., S. SAWAYA, T. H. VINES, A. K. KNECHT, C. T. MILLER *et al.*, 2008 The genetics of adaptive shape shift in stickleback: pleiotropy and effect size. Evolution **62:** 76-85.

ANKER, G. C., 1974 Morphology and kinetics of the head of the stickleback, *Gasterosteus aculeatus*. Trans. Zool. Soc. Lond. **32:** 311-416.

BROMAN, K. W., and S. SEN, 2009 *A guide to QTL mapping with R/qtl*. Springer, Dordrecht.

BURKE, J. M., S. TANG, S. J. KNAPP and L. H. RIESEBERG, 2002 Genetic analysis of sunflower domestication. Genetics **161:** 1257-1267.

COLOSIMO, P. F., K. E. HOSEMANN, S. BALABHADRA, G. VILLARREAL, JR., M. DICKSON *et al.*, 2005 Widespread parallel evolution in sticklebacks by repeated fixation of *Ectodysplasin* alleles. Science **307:** 1928-1933.

COLOSIMO, P. F., C. L. PEICHEL, K. NERENG, B. K. BLACKMAN, M. D. SHAPIRO *et al.*, 2004 The genetic architecture of parallel armor plate reduction in threespine sticklebacks. PLoS Biol **2:** e109.

GHANEM, N., O. JARINOVA, A. AMORES, Q. LONG, G. HATCH *et al.*, 2003 Regulatory roles of conserved intergenic domains in vertebrate *Dlx* bigene clusters. Genome Res **13:** 533-543.

JONES, F. C., M. G. GRABHERR, Y. F. CHAN, P. RUSSELL, E. MAUCELI *et al.*, 2012 The genomic basis of adaptive evolution in threespine sticklebacks. Nature **484:** 55-61.

KINGSLEY, D. M., B. L. ZHU, K. OSOEGAWA, P. J. DE JONG, J. SCHEIN *et al.*, 2004 New genomic tools for molecular studies of evolutionary change in threespine sticklebacks. Behaviour **141:** 1331-1344.

KNECHT, A. K., K. E. HOSEMANN and D. M. KINGSLEY, 2007a Constraints on utilization of the EDA-signaling pathway in threespine stickleback evolution. Evolution & Development **9:** 141-154.

KNECHT, A. K., K. E. HOSEMANN and D. M. KINGSLEY, 2007b Constraints on utilization of the EDA-signaling pathway in threespine stickleback evolution. Evol Dev **9:** 141-154.

MILLER, C. T., S. BELEZA, A. A. POLLEN, D. SCHLUTER, R. A. KITTLES *et al.*, 2007 *cis*-Regulatory changes in *Kit ligand* expression and parallel evolution of pigmentation in sticklebacks and humans. Cell **131:** 1179-1189.

PEICHEL, C. L., K. S. NERENG, K. A. OHGI, B. L. COLE, P. F. COLOSIMO *et al.*, 2001 The genetic architecture of divergence between threespine stickleback species. Nature **414:** 901-905.

SHAPIRO, M. D., M. E. MARKS, C. L. PEICHEL, B. K. BLACKMAN, K. S. NERENG *et al.*, 2004 Genetic and developmental basis of evolutionary pelvic reduction in threespine sticklebacks. Nature **428:** 717-723.

ZERUCHA, T., T. STUHMER, G. HATCH, B. K. PARK, Q. LONG *et al.*, 2000 A highly conserved enhancer in the *Dlx5/Dlx6* intergenic region is the site of cross-regulatory interactions between *Dlx* genes in the embryonic forebrain. J Neurosci **20:** 709-721.